Global trends in surface ocean pCO_2 from in situ data

A. R. Fay[1] and G. A. McKinley[1]

Received 3 August 2012; revised 14 May 2013; accepted 17 May 2013; published 20 June 2013.

[1] Ocean carbon uptake substantially reduces the rate of anthropogenic carbon accumulation in the atmosphere and thus slows global climate change. In the interest of understanding how this ocean carbon sink has responded to climate variability and climate change in recent decades, trends in globally observed surface ocean partial pressure of CO_2 ($pCO_2^{s.ocean}$) are evaluated over 16 gyre-scale biomes covering the globe. Trends from decadal to multidecadal timescales between 1981 and 2010 are considered. On decadal timescales, $pCO_2^{s.ocean}$ trends have been of variable magnitude and sensitive to the chosen start and end years. On longer time frames, several regions of the tropics and subtropics display $pCO_2^{s.ocean}$ trends that are parallel to or shallower than trends in atmospheric pCO_2, consistent with the ocean's long-term response to carbon accumulation in the atmosphere and with the supply of waters with low anthropogenic carbon from the deep ocean. Data are too sparse in the high latitudes to determine this long-term response. In many biomes, $pCO_2^{s.ocean}$ trends steeper than atmospheric trends do occur on shorter timescales, which is consistent with forcing by climatic variability. In the Southern Ocean, the influence of a positive trend in the Southern Annular Mode has waned and the carbon sink has strengthened since the early 2000s. In North Atlantic subtropical and equatorial biomes, warming has become a significant and persistent contributor to the observed increase in $pCO_2^{s.ocean}$ since the mid-2000s. This long-term warming, previously attributed to both multidecadal climate variability and anthropogenic forcing, is beginning to reduce ocean carbon uptake.

Citation: Fay, A. R., and G. A. McKinley (2013), Global trends in surface ocean pCO_2 from in situ data, *Global Biogeochem. Cycles*, *27*, 541–557, doi:10.1002/gbc.20051.

1. Introduction

[2] Since the industrial revolution, atmospheric carbon dioxide levels have increased dramatically. At the end of 2010, the global atmospheric concentration was 390 ppm, over 30% higher than pre-1850 [*Peters et al.*, 2011]. This change is due to human activities, specifically the burning of fossil fuels, cement production, and land use changes [*Keeling and Whorf*, 2005]. Only 43% of anthropogenic carbon has remained in the atmosphere [*Le Quéré et al.*, 2009], with the rest absorbed into terrestrial and oceanic sinks. Land use and biomass burning have led to a net terrestrial flux of CO_2 to the atmosphere over the past 200 years [*Khatiwala et al.*, 2009], leaving the oceans to serve as the only long-term net sink. Were it not for oceanic uptake, atmospheric CO_2 would be 55–75 ppm higher than present [*Sabine et al.*, 2004; *Khatiwala et al.*, 2012].

Additional supporting information may be found in the online version of this article.

[1]Department of Atmospheric and Oceanic Sciences, University of Wisconsin-Madison, Madison, Wisconsin, USA.

Corresponding author: A. R. Fay, Department of Atmospheric and Oceanic Sciences, University of Wisconsin-Madison, 1225 W. Dayton St., Madison, WI 53706, USA. (arfay@wisc.edu)

©2013. American Geophysical Union. All Rights Reserved.
0886-6236/13/10.1002/gbc.20051

[3] Due to ever increasing anthropogenic emissions, atmospheric CO_2 concentrations continue to rise and trigger climate change [*Solomon et al.*, 2007; *Le Quéré et al.*, 2009; *Peters et al.*, 2011]. The response of the ocean carbon sink to increasing atmospheric CO_2, and to the climate change that it drives, must be diagnosed in the interest of understanding the global carbon cycle and projecting its future response to continued anthropogenic forcing. Modeling suggests that changes in wind stress and warming will be the first climate-driven negative feedbacks on the ocean carbon sink [*Sarmiento and Le Quéré*, 1996; *Le Quéré et al.*, 2010; *Roy et al.*, 2011]. It is important to determine if these impacts can already be identified from existing data.

[4] The partial pressure of CO_2 in the surface ocean ($pCO_2^{s.ocean}$) controls the direction and long-term magnitude of the ocean's carbon uptake. The $pCO_2^{s.ocean}$ is determined by the sea surface temperature (SST), total CO_2 concentration (TCO_2), alkalinity (ALK), and sea surface salinity (SSS), which, in turn, can be modified by air-sea fluxes of heat and freshwater, circulation changes, and biological activity. Basic thermodynamics tell us that the global mean $pCO_2^{s.ocean}$ should tend toward equilibrium with atmospheric pCO_2 on long timescales. Yet regionally, the effects of ocean circulation and biology cause certain regions to be persistent sinks and others persistent sources [*Takahashi et al.*, 2009; *Gruber et al.*, 2009]. Thus, if ocean circulation and biology were to be unchanged through time,

the slope of $pCO_2^{s.ocean}$ trends should parallel the trend in atmospheric pCO_2 (pCO_2^{atm}). As a corollary, if $pCO_2^{s.ocean}$ trends are shallower or steeper than the pCO_2^{atm} trend, variability in ocean circulation and biology can be inferred.

[5] Previous studies have interpreted observed $pCO_2^{s.ocean}$ trends steeper than the pCO_2^{atm} trend as a declining ocean carbon sink. This is because the ΔpCO_2 ($pCO_2^{atm} - pCO_2^{s.ocean}$), which is the driving force for the CO_2 uptake, is assumed to have been decreasing over time. Similarly, a $pCO_2^{s.ocean}$ trend shallower than the pCO_2^{atm} trend has been interpreted as an increasing sink, and a parallel trend has been interpreted as a constant sink. Yet, this interpretation ignores the fact that $pCO_2^{s.ocean}$ not only drives the CO_2 sink (via ΔpCO_2) but also responds to the air-sea CO_2 flux. In this study, we avoid these interpretations. Previous studies have also assumed that the entire trend in $pCO_2^{s.ocean}$ has been driven by the accumulation of anthropogenic CO_2, ignoring an unquantified component due to surface ocean warming, which numerical models have predicted to be a significant influence in this century [*Sarmiento and Le Quéré*, 1996; *Le Quéré et al*., 2010; *Roy et al*., 2011]. In this study, we quantify this warming component and interpret a significant contribution of warming to trends in $pCO_2^{s.ocean}$ as a negative feedback on ocean carbon uptake.

[6] On a regional scale, significant debate is ongoing regarding the Southern Ocean sink [*Lovenduski et al*., 2007, 2008; *Le Quéré et al*., 2007, 2009; *Böning et al*., 2008; *Ito et al*., 2010; *Lenton et al*., 2012]. Several studies, based primarily on numerical models, suggest that a transition to a positive Southern Annular Mode (SAM) in recent decades has caused a poleward shift in the westerlies and increased upwelling of natural carbon [*Le Quéré et al*., 2007; *Lovenduski et al*., 2007, 2008]; however, accurate modeling of circulation changes continues to be a challenge. Eddy-resolving models show that intra-annual variability in the northward transport of anthropogenic carbon is dominated by Ekman processes [*Ito et al*., 2010], while longer-term coarse-resolution modeling suggests a strong dependence on eddy processes that are poorly represented [*Böning et al*., 2008]. In the North Atlantic, studies using mostly Volunteer Observing Ship $pCO_2^{s.ocean}$ observations have suggested substantial declines in the CO_2 sink, but these have been limited in the spatial extent to which they directly apply [*Corbière et al*., 2007; *Schuster and Watson*, 2007; *Watson et al*., 2009; *Schuster et al*., 2009; *Metzl et al*., 2010]. North Atlantic modeling studies that span the whole basin suggest that decadal variability is a significant component of these apparent trends [*Thomas et al*., 2008; *Ullman et al*., 2009]. Globally, *Le Quéré et al*. [2009] analyzed trends in $pCO_2^{s.ocean}$ in $5° \times 5°$ regions where data in at least 3 decades are colocated. For 1981–2007, they find that trends in North Pacific $pCO_2^{s.ocean}$ were shallower than the pCO_2^{atm} trend and trends in the North Atlantic $pCO_2^{s.ocean}$ were steeper than the pCO_2^{atm} trend. Outside these regions, *Le Quéré et al*. [2009] have only very limited locations where their method can be applied.

[7] One concern with studies of trends in $pCO_2^{s.ocean}$ is the sensitivity of trend estimates to the years included in the analysis due to variability internal to the ocean or forced from the atmosphere. The annual growth rate of atmospheric CO_2 varies considerably more than estimated anthropogenic CO_2 emissions, indicating that the variability of carbon sinks is significant. Ocean variability has been linked to ocean temperature, chemistry, and circulation [*Peylin et al*., 2005; *McKinley et al*., 2004; *Thomas et al*., 2008; *Ullman et al*., 2009; *Le Quéré et al*., 2010]. The degree to which this interannual to decadal timescale climate variability obscures long-term trends in $pCO_2^{s.ocean}$ must be understood.

[8] To address the needs highlighted above, *McKinley et al*. [2011] developed a methodology for estimating trends in the carbon sink over three large biogeographical regions in the North Atlantic. They applied this method to a range of time frames spanning 9 to 29 years, in order to distinguish long-term trends from interannual to decadal timescale variability. In this paper, we apply the approach of *McKinley et al*. [2011] to the global ocean using a vast, newly updated, in situ $pCO_2^{s.ocean}$ data set [*Takahashi et al*., 2011]. We determine the trends, and the driving mechanisms of these trends, in the ocean carbon sink over 16 gyre-scale biomes and for the time series of lengths varying from 4 to 30 years. In so doing, we are able to distinguish decadal variations due to climatic oscillations from long-term changes in the carbon sink.

2. Methodology

2.1. Global Biomes

[9] We estimate trends over physical biologically defined regions [*Sarmiento et al*., 2004] or "biomes" (Figure 1a) delineated based on three climatological criteria: maximum mixed layer depth (MLD), chlorophyll *a* (Chl), and sea surface temperature (SST) (Table S1 in the supporting information). MLD values are calculated from the World Ocean Atlas using a surface to depth density difference of 0.125 kg/m^3 [*Antonov et al*., 2006]. Due to insufficient coverage in the climatology, especially in the Southern Hemisphere, grid cells missing monthly MLD values are assigned the latitudinal mean. Annual mean chlorophyll *a* is obtained from SeaWiFS, averaged over years 1998 to 2008. The SST climatology is from the Hadley Centre Sea Ice and Sea Surface Temperature data set (HADISST) [*Rayner et al*., 2003], averaged over years 1981–2010.

[10] Cooler waters that have ice cover during some part of the year are grouped into the marginal sea ice (ICE) biome, with average temperatures <4°C. Subpolar seasonally stratified (SPSS) biomes have divergent surface flow driven by the positive wind stress curl (i.e., upwelling), allowing for higher chlorophyll concentrations due to continual nutrient resupply. The subtropical seasonally stratified (STSS) biome is an area of downwelling due to negative wind stress curl, but intermediate chlorophyll concentrations due to deep winter MLDs. The subtropical permanently stratified (STPS) biome experiences negative wind stress curl, leading to convergence and stratification, such that MLDs are shallow and Chl is low. Equatorial biomes (EQU) are between 5°S and 5°N. In the Indian Ocean, the equatorial region is grouped in with the STPS biome due to seasonally varying physical ocean circulation patterns linked to the monsoon. A biome for middle- and low-latitude upwelling regions could also be defined [*Sarmiento et al*., 2004], but $pCO_2^{s.ocean}$ data are too scarce for this analysis.

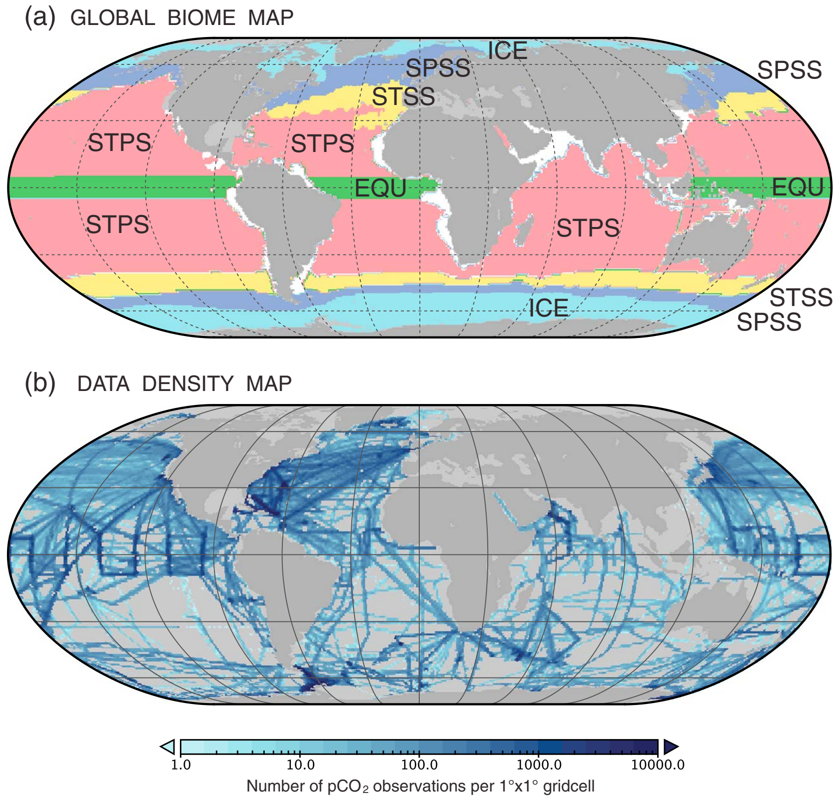

Figure 1. Maps of (a) global biomes and (b) global data density in the *Takahashi et al*. [2011] database. From north to south in Figure 1a, the global biomes include the ice biomes (ICE), subpolar seasonally stratified biomes (SPSS), subtropical seasonally stratified biomes (STSS), subtropical permanently stratified biomes (STPS), and equatorial biomes (EQU) for each ocean basin.

2.2. Data Sources and Treatment

[11] The Takahashi LDEO database of direct global $pCO_2^{s.ocean}$ measurements made using air-seawater equilibration methods (V2010; downloaded June 2011 from http://cdiac.ornl.gov/oceans/LDEO_Underway_Database/index.html) is our primary data set. These data cover the world ocean but are biased spatially to the Northern Hemisphere (Figure 1b). *Takahashi et al*. [2011] described the compilation and initial quality control measures. The average precision is estimated at ±2.5 μatm. Data collected during El Niño events are retained. The database is supplemented with data collected along ship tracks between Iceland and Newfoundland [*Corbière et al*., 2007; *Metzl*, 2009], as in *McKinley et al*. [2011]. These additional 1155 observations fill temporal gaps in the database, particularly in 2001–2002. Additionally, data collected onboard R/V *Ka'imimoana* during 2007 and 2008 cruises are added to our data set [*Feely and Sabine*, 2007, 2008].

[12] In the combined $pCO_2^{s.ocean}$ data set, coastal influences were eliminated by excluding data with SSS values of less than or equal to 20 psu, which reduced the observations by roughly 25,000. After this elimination, 757,000 remaining points, roughly 10%, fall outside the biomes and were not further considered. The remaining 4,761,747 data points span years 1957 thru 2010, and 4,474,891 (94%) fall between 1981 and 2010. Additional outliers in $pCO_2^{s.ocean}$ are detected by removing points associated with SST anomalies that fall outside 3 standard deviations from HADISST. Depending on the biome, from 4 to 163 points are removed in this way, with an average of 41. After this SST-based quality control, data are averaged to monthly mean at $1° \times 1°$ resolution.

[13] Atmospheric xCO_2 values are obtained from NOAA ESRL GLOBALVIEW-CO2 reference marine boundary layer matrix [*GLOBALVIEW-CO2*, 2010]. We convert these interpolated xCO_2 monthly mean values, regridded at $1° \times 1°$ resolution, to pCO_2^{atm} with NCEP/NCAR reanalysis monthly mean sea level pressure, also taking into account a surface vapor pressure correction [*Weiss and Price*, 1980] calculated from monthly HADISST [*Rayner et al*., 2003] and WOA salinity climatology [*Antonov et al*., 2006]. Climatologies of $pCO_2^{s.ocean}$ [*Takahashi et al*., 2009] and SST, as used in biome definition, are also employed; both regridded to $1° \times 1°$ resolution.

[14] In section 4, results are interpreted in the context of several climate indices. The Pacific Decadal Oscillation (PDO) index [*Mantua et al*., 1997] is from JISAO/University of Washington. The Niño3.4 El Niño/Southern Oscillation (ENSO) index, as well as the Southern Annular Mode (SAM), or Antarctic Oscillation (AAO), is from NOAA's Climate Prediction Center (CPC). Results for CPC-based SAM trends did not differ significantly from an alternative station-based index by the British Antarctic Survey-Natural Environmental Research Council (NERC-BAS). We also use the North Atlantic Oscillation (NAO) index [*Hurrell and Deser*, 2010] produced by NOAA-CPC and the Atlantic Multidecadal Variation (AMV), or Atlantic Multidecadal Oscillation, from NOAA's Earth System Research Laboratory.

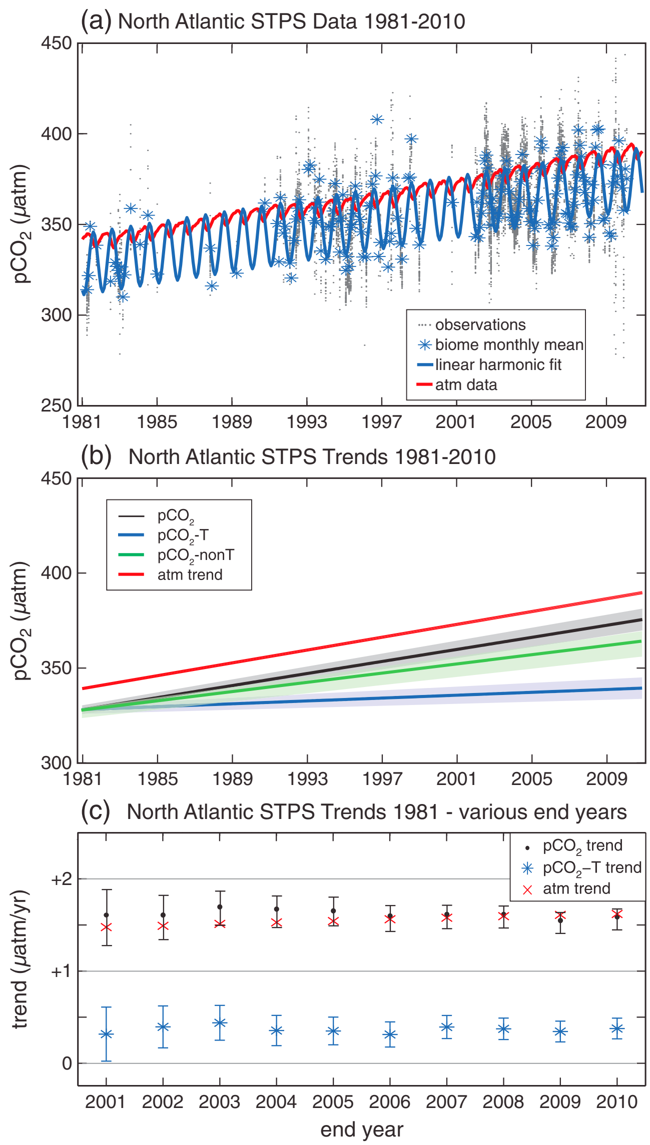

Figure 2. Time series for the North Atlantic subtropical permanently stratified biome (NA-STPS). (a) Time series showing individual in situ $pCO_2^{s.ocean}$ observations (black dots), monthly means (stars), the linear harmonic fit to the data (blue line), and the corresponding atmospheric monthly means for the biome (red line). (b) Estimated trends in $pCO_2^{s.ocean}$ for 1981–2010 (black line; 1σ uncertainties shaded), pCO_2^{atm} (red line), temperature (pCO_2-T; blue line), and chemical (pCO_2-nonT; green line) components. In this example, the pCO_2-T trend is statistically distinguishable from zero. For visual clarity, the pCO_2-T and pCO_2-nonT trends are shifted vertically to have the same intercept as $pCO_2^{s.ocean}$. (c) Estimated trends, and uncertainty, in $pCO_2^{s.ocean}$ (black dots), pCO_2^{atm} (red crosses), and pCO_2-T (blue stars) for 10 time series, start year 1981, and end years 2001 through 2010 (x axis). This figure illustrates the change in the $pCO_2^{s.ocean}$ trend as the time series lengthen, as well as the decrease in uncertainty. In all 10 time series, the $pCO_2^{s.ocean}$ trend is indistinguishable from the pCO_2^{atm} trend given their uncertainties, i.e., a *parallel* trend. The pCO_2-T trends are greater than zero, indicating a warming influence on the $pCO_2^{s.ocean}$ trend.

2.3. Fitting of Harmonic Function and Linear Trend

[15] Trends in $pCO_2^{s.ocean}$ and pCO_2^{atm} are calculated in four steps.

[16] 1. Global data are averaged to 1° × 1° spatial and monthly temporal resolution.

[17] 2. The long-term mean $pCO_2^{s.ocean}$ [*Takahashi et al.*, 2009] for each 1° × 1° cell is removed to eliminate spatial aliasing prior to analyzing over large regions.

[18] 3. Monthly anomalies are averaged spatially across each of the 16 biomes.

[19] 4. A harmonic of the form $y = a + b \times t + c \times \cos(2\pi t + d)$, where t is the decimal year -1981, is fit to capture both a sinusoidal annual cycle and linear trend for data in each biome (Figure 2a).

[20] Trends reported in our analysis are the value of the coefficient b (in μatm/yr). Uncertainty in the calculated trends is presented here as the 1σ confidence intervals (68.3%) for the resulting $pCO_2^{s.ocean}$ and pCO_2^{atm} trends using

$$CI_b = \pm t \times RMSE \times \sqrt{\frac{1}{\sum (X_i - \overline{X})^2}}$$

where t is the two-tailed t statistic for 68.3% confidence for $N-4$ degrees of freedom (DOF), with N being the number of months [*Wilks*, 2006]. RMSE is the root-mean-square error, X_i are the data, and $\overline{X}$ is the mean value. For $pCO_2^{s.ocean}$, the 1981–2010 16-biome average CI^b is 0.2 μatm/yr, much larger than that for pCO_2^{atm} (0.01 μatm/yr). This is in part because temporal coverage is far greater for pCO_2^{atm}. However, if the trend is calculated from pCO_2^{atm} sampled as $pCO_2^{s.ocean}$, the average CI_b increases to only 0.02 μatm/yr, indicating that the well-mixed atmosphere is most important to the small CI_b for pCO_2^{atm}.

[21] For each biome, this analysis is repeated for each possible combination of 18 start years (1981–1998) and 10 end years (2001–2010), leading to a total of 180 linear trends in $pCO_2^{s.ocean}$ and pCO_2^{atm} for each biome (Figures 5–7). For each time series, distinguishability between the $pCO_2^{s.ocean}$ and pCO_2^{atm} trends is determined by Student's t-test with t^* calculated from the data using

$$t^* = \frac{b_{s.ocean} - b_{atm}}{\sigma_e / S_{xx}}$$

where $b_{s.ocean}$ is the surface ocean trend, b_{atm} is the atmospheric trend, σ_e is the sum of squared errors divided by the DOF, and S_{xx} is calculated by

$$\sum_i^N (x_i - \overline{x})^2$$

[22] If t^* is greater than $T_{(0.683)}$ given the DOF, then the atmospheric and $pCO_2^{s.ocean}$ trends are significantly different. If $t^* < T_{(0.683)}$, then the trends are not significantly different [*von Storch and Zwiers*, 2002]. Histograms of residuals are normally distributed and monthly time series pass a test of kurtosis.

[23] *Jones et al.* [2012] found that seasonal variability dominates the autocorrelation in these $pCO_2^{s.ocean}$ data, with a 12 month global mean autocorrelation of 0.46. Consistent with this, we find very low autocorrelation once the seasonal cycle has been removed. The global average autocorrelation for 1–12 month lag is 0.04, and thus, we do not further consider autocorrelation.

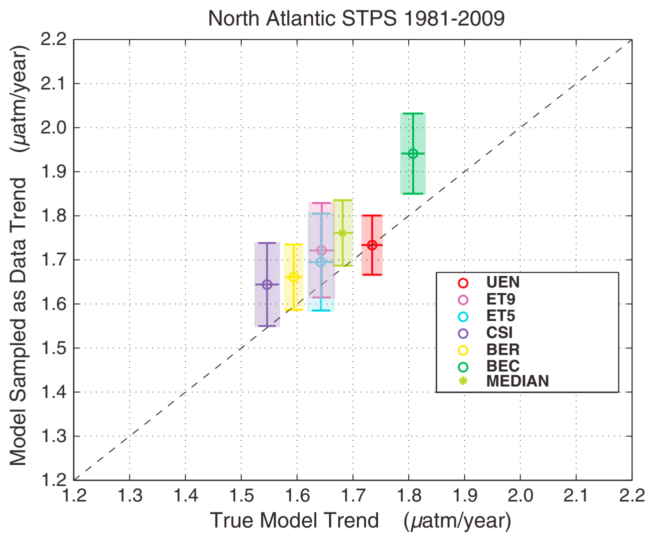

Figure 3. Evaluation of data representativity for the biomes with 1981–2009 for NA-STPS as an example. Trends from the full and sampled models (circles), with 1σ uncertainty regions (bars and shaded boxes), and the median model (star). If the shaded area intersects the 1:1 line (dashed line), the two estimates are indistinguishable. In order to be confirmed, the sampled and true trends from at least half the individual models, as well as from the ensemble median, must be indistinguishable in this way. This confirmation is repeated for each of the 180 time series in each biome.

2.4. Interpretation

[24] The difference between $pCO_2^{s.ocean}$ and pCO_2^{atm} (ΔpCO_2) determines the direction of the flux of carbon between the ocean and atmosphere. If a $pCO_2^{s.ocean}$ trend is less than the pCO_2^{atm} trend and their 1σ uncertainties do not overlap, the ocean trend is said to be *shallower* than the atmosphere, corresponding to an increase in ΔpCO_2 over the time series [*Le Quéré et al.*, 2009]. If the $pCO_2^{s.ocean}$ trend is greater than the pCO_2^{atm} trend, this is a *steeper* $pCO_2^{s.ocean}$ trend or a decline in ΔpCO_2 over the time series. *Parallel* trends occur when the $pCO_2^{s.ocean}$ and pCO_2^{atm} trends are statistically indistinguishable given their uncertainties (Figure 2b). In this case ΔpCO_2 would remain constant.

[25] Without changing ocean biology and circulation, the long-term mean spatial pattern of ΔpCO_2 should persist such that regional $pCO_2^{s.ocean}$ trends generally track pCO_2^{atm} trends and the global mean $pCO_2^{s.ocean}$ tends toward pCO_2^{atm}. Yet, ocean biology and circulation are not constant, and thus, we interpret shallower and steeper $pCO_2^{s.ocean}$ trends on multiyear timescales as evidence of the impact of this variability on surface ocean carbon. In regions of significant mixing with or upwelling from the abyssal ocean, shallower $pCO_2^{s.ocean}$ trends can also indicate the supply of waters with low anthropogenic carbon from depth.

[26] We also determine the driving mechanisms of the ocean carbon trend via a decomposition of $pCO_2^{s.ocean}$ trends into two components: the isochemical component due to temperature (pCO_2-T) and the remaining variability (pCO_2-nonT), due to biological and chemical factors SSS, ALK, and TCO_2, using the empirical equations of *Takahashi et al.* [2002]:

$$\mathrm{pCO_2\text{-}T} = \text{mean } pCO_2 \times \exp(0.0423 \times (\text{observed } SST - \text{mean } SST))$$

$$\mathrm{pCO_2\text{-}nonT} = \text{observed } pCO_2 \times \exp(0.0423 \times (\text{mean } SST - \text{observed } SST))$$

[27] In their seasonality and interannual variability, these two effects (pCO_2-T and pCO_2-nonT) can often act in opposition to one another, particularly at high latitudes [*Gruber et al.*, 2002; *Takahashi et al.*, 2002; *McKinley et al.*, 2004, 2006; *Bennington et al.*, 2009; *Ullman et al.*, 2009]. In terms of trends due to the accumulation of anthropogenic carbon in the ocean [*Khatiwala et al.*, 2012], pCO_2-nonT typically dominates the $pCO_2^{s.ocean}$ trend (Figure 2b). However, pCO_2-T also can contribute to trends. In these cases, warming temperatures are a contributing factor to the rise in $pCO_2^{s.ocean}$, such that less carbon is absorbed from the atmosphere than if pCO_2-nonT were the only component driving the $pCO_2^{s.ocean}$ trend, for example, North Atlantic STPS for all time series with a start year of 1981 (Figures 2b and 2c). In Figure 2c, we use the North Atlantic subtropical permanently stratified (NA-STPS) biome as an example to show linear trends, and corresponding uncertainties, in $pCO_2^{s.ocean}$, pCO_2^{atm}, and pCO_2-T for 10 time series, all with a start year of 1981 and end years ranging from 2001 to 2010 (*x* axis). For each of the 10 time series considered, $pCO_2^{s.ocean}$ trends parallel trends to pCO_2^{atm} (black dots and red crosses). In addition, for all 10, the pCO_2-T trend (blue star) is distinguishably greater than zero, indicating a significant contribution from warming temperatures to the $pCO_2^{s.ocean}$ trend.

[28] In Figures 5–7, $pCO_2^{s.ocean}$ and pCO_2^{atm} trends for all biomes and all 180 time series are compared. Each cell in the grids represents a different time series (*y* axis: start year; *x* axis: end year) of pCO_2 data. The color denotes the slope of the $pCO_2^{s.ocean}$ trend as compared to the slope of pCO_2^{atm} (red: steeper; pink: parallel; dark blue: shallower). The shading indicates time series that present a trend in pCO_2-T statistically different from zero. Results in Figure 2c are the same as in the top row of Figure 6d.

2.5. Model Confirmation

[29] In order to verify that biome-scale $pCO_2^{s.ocean}$ trends are robust despite the highly variable spatial and temporal data coverage, we perform tests using a collection of realistic hindcast general circulation models with embedded biogeochemistry from the Regional Carbon Cycle Assessment and Processes (RECCAP) project [*Canadell et al.*, 2011; *Schuster et al.*, 2012]. Six global models are employed in this analysis: the Community Climate System Model (CCSM-BEC) [*Doney et al.*, 2009]; the NEMO-PlankTOM5 (UEN) produced by the University of East Anglia [*Buitenhuis et al.*, 2010]; the Bergen earth system model (BER) [*Assmann et al.*, 2010]; the global 3-D biogeochemical ocean general circulation model produced by the Commonwealth Scientific and Industrial Research Organisation (CSI) [*Matear and Hirst*, 2003]; and, finally, two models, produced by ETH Zurich, which use two different gas transfer velocities (ET5 and ET9) [*Smith and Gent*, 2002; *Graven et al.*, 2012]. All model results are available for 1981–2009, except ET5 and ET9, which are 1981–2007. Since we do not have any model output for the year 2010, results for 1981–2009 are applied to 1981–2010 time series.

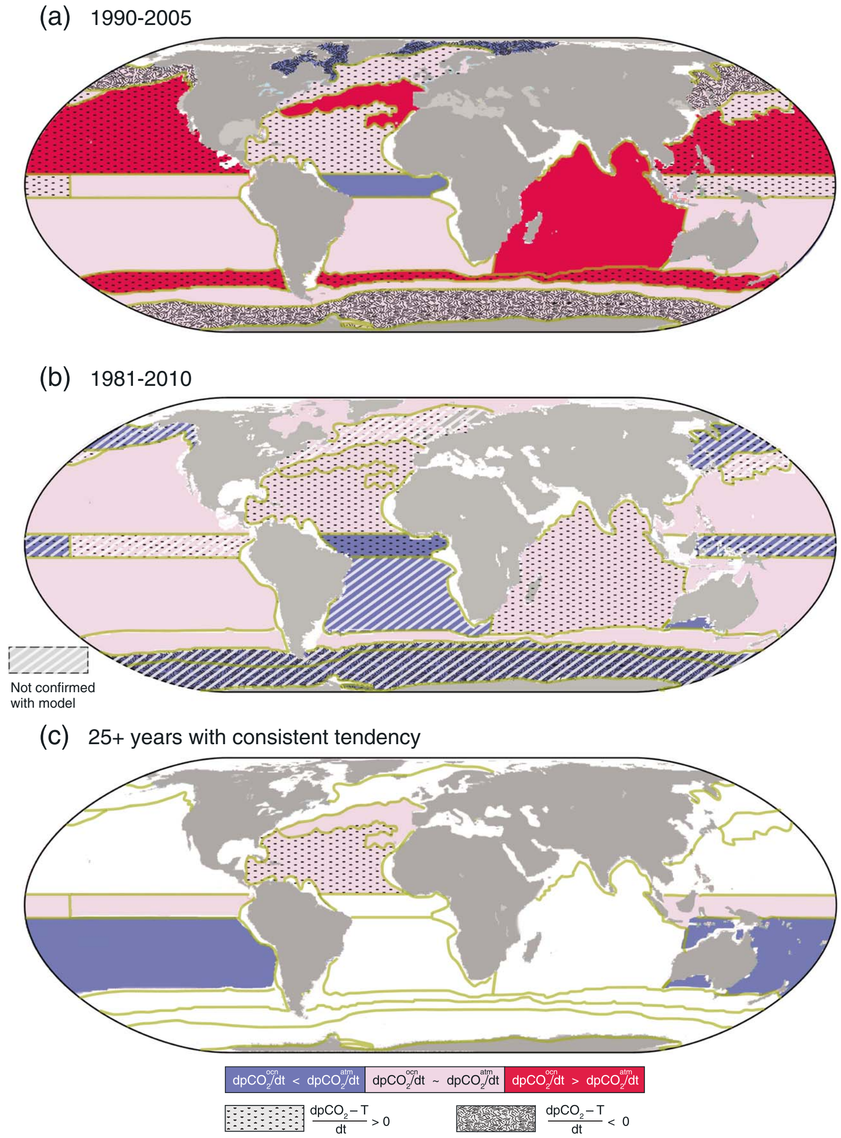

Figure 4. Global biome maps showing trends in $pCO_2^{s.ocean}$ for (a) 1990–2005 and (b) 1981–2010 compared to the pCO_2^{atm} trend, with white stripes for biomes with unconfirmed trends (see section 2.4), and (c) for the biomes where a majority (>64%) of trends for 25+ year time series both are confirmed by models and give the same signal when compared to the pCO_2^{atm} trend. Dark blue for the $pCO_2^{s.ocean}$ trend shallower than the pCO_2^{atm} trend, pink for parallel, and red for steeper $pCO_2^{s.ocean}$ trend. Stippling for the pCO_2-T trend significantly different from zero (dot: >0; dark: <0).

[30] Each model is sampled as the data, and a "sampled" trend is estimated for each biome and each time frame using the methodology outlined in section 2.3. This "sampled" model trend is compared to the trend from all model output, the "true" model trend. Also, a median model sampled (true) trend is calculated from the median monthly sampled (true) pCO_2 value from these six models. The average difference between sampled and true model trends for all biomes is -0.033 μatm/yr.

[31] A biome is considered "confirmed" if, for that biome and that time frame, at least half of the global climate models, as well as the median, captures the full model trend within 1σ uncertainty bounds. In Figure 3, this process for 1981–2009 in the NA-STPS biome is presented graphically. This time series is confirmed because the criteria above are met. We test for "confirmation" for each combination of start and end years in each biome. The whited-out areas in Figures 5–7 are the time series not confirmed in this way.

3. Results

[32] The $pCO_2^{s.ocean}$ trends are compared to the pCO_2^{atm} trends for a variety of timescales, ranging from 4 years (1998–2001) to 30 years (1981–2010). By comparing trends over varying timescales, influences of climatic variability on interannual to decadal timescales, as driven by major climate indices such as ENSO or NAO, are revealed. In addition, a determination of where and on what timescales there is evidence of the response of the ocean sink to anthropogenic CO_2 loading in the atmosphere and, in some cases, feedbacks of climate change on the ocean carbon sink can be made.

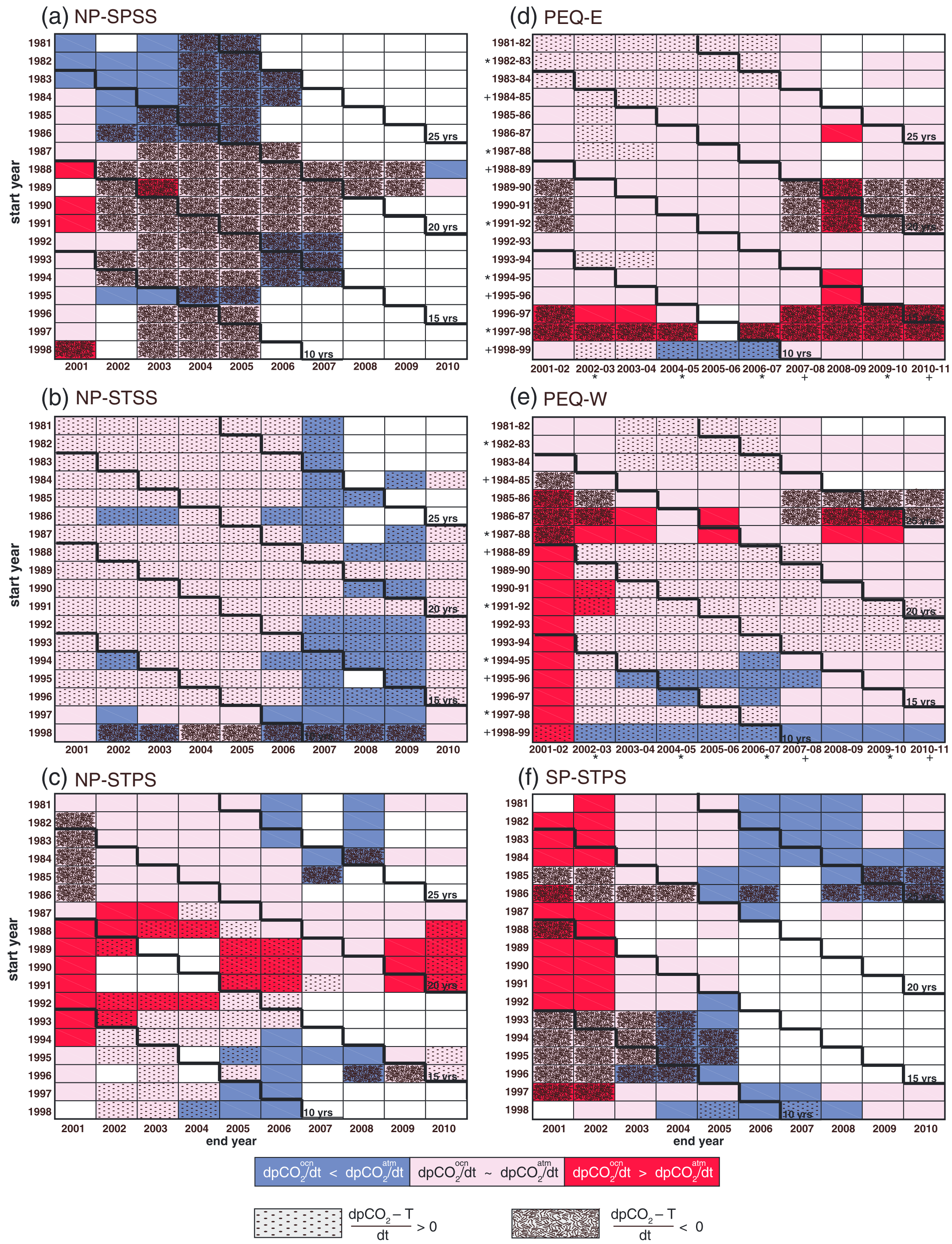

Figure 5. Trend in $pCO_2^{s.ocean}$ versus pCO_2^{atm} for 180 different time series, with start (y axis) and end (x axis) years. Dark blue for the $pCO_2^{s.ocean}$ trend shallower than the pCO_2^{atm} trend, pink for parallel, and red for steeper $pCO_2^{s.ocean}$ trend. Stippling for the pCO_2-T trend distinguishable from zero (dot: > 0; dark: < 0). Pacific Ocean biomes: (a) subpolar seasonally stratified (NP-SPSS), (b) subtropical seasonally stratified (NP-STSS), (c) subtropical permanently stratified (NP-STPS), (d) eastern equatorial (PEQ-E), (e) western equatorial (PEQ-W), and (f) subtropical permanently stratified (SP-STPS). Bold lines at time series of 10, 15, 20, and 25 years in length. In Figures 5d and 5e, the stars signify El Niño years and the crosses signify La Niña events. White indicates that the time series is not confirmed by models (section 2.4). Figure S1 is the same without white shading.

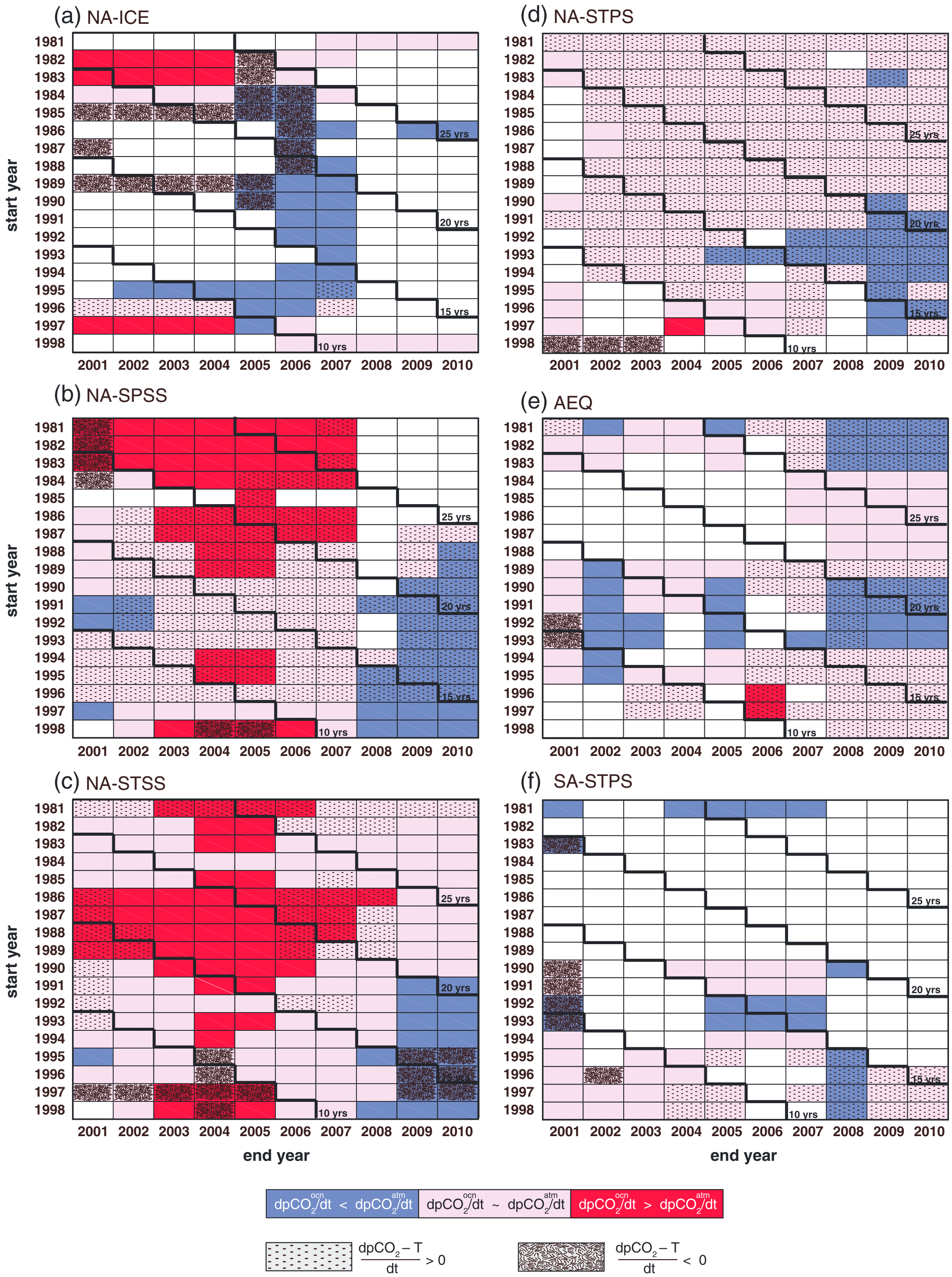

Figure 6. Trend in $pCO_2^{s.ocean}$ versus pCO_2^{atm} trend, with variable start and end years for Atlantic Ocean biomes: (a) ice (NA-ICE), (b) subpolar seasonally stratified (NA-SPSS), (c) subtropical seasonally stratified (NA-STSS), (d) subtropical permanently stratified (NA-STPS), (e) equatorial (AEQ), and (f) subtropical permanently stratified (SA-STPS). Colors and stippling as in Figure 4. White indicates that the time series is not confirmed by models (section 2.4). See also Figure S2.

[33] We begin with one example of a 16 year time series, 1990–2005, for the global biomes (Figure 4a). Shallower, parallel, and steeper trends are all found across the global biomes, and significant influences of both warming and cooling are also evident. In contrast, on the longest time series for which we have sufficient data, 1981–2010, $pCO_2^{s.ocean}$ trends parallel those of pCO_2^{atm} in seven out of the eight confirming biomes (Figure 4b). The total magnitude of $pCO_2^{s.ocean}$ trends is due primarily to the changing chemistry of the surface ocean (pCO_2-nonT) in all biomes.

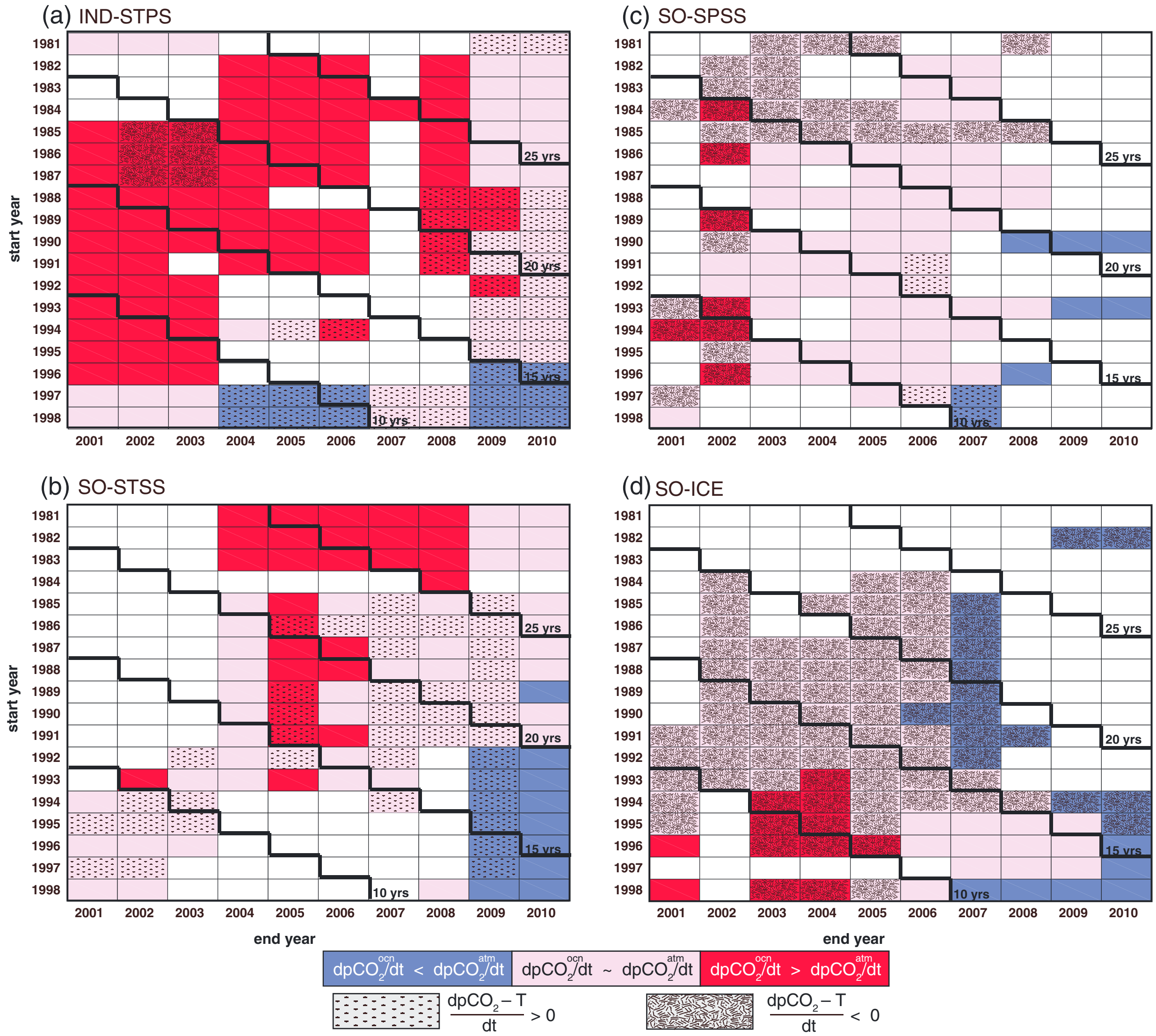

Figure 7. Trend in $pCO_2^{s.ocean}$ versus pCO_2^{atm} trend, with variable start and end years for Indian Ocean and Southern Ocean biomes: (a) Indian Ocean subtropical permanently stratified (IND-STPS), (b) Southern Ocean subtropical seasonally stratified (SO-STSS), (c) Southern Ocean subpolar seasonally stratified (SO-SPSS), and (d) Southern Ocean ice (SO-ICE). Colors and stippling as in Figure 4. White indicates that the time series is not confirmed by models (section 2.4). See also Figure S3.

However, there is a significant contribution to the 1981–2010 oceanic pCO_2 trend from rising temperatures (pCO_2-T) in the North Atlantic subtropical seasonally stratified (NA-STSS), North Atlantic subtropical permanently stratified (NA-STPS), Atlantic equatorial (AEQ), and Indian Ocean subtropical permanently stratified (IND-STPS) biomes (Figure 4b, dotted, without white slash). That the decadal timescale result is so distinct from those for 1981–2010 suggests that the results for 1990–2005 are significantly influenced by decadal timescale variability. In Figure 4c, only the five biomes that have a consistent signal of steeper, parallel, or shallower $pCO_2^{s.ocean}$ trends for all time series at least 25 years long (top right corner of Figures 5–7) and that are confirmed with the model test are shown. Most biomes do not have enough data to meet these criteria. For each biome, we now consider in detail the $pCO_2^{s.ocean}$ trends across time series of 4–30 years and then return to a global interpretation in section 5.

3.1. Pacific Ocean

[34] Both North Pacific high-latitude biomes (NP-SPSS and NP-STSS; Figures 5a and 5b) have poor confirmation on long timescales, with less than half of time series of 25 years or longer confirming. For start/end year pairs that do confirm, $pCO_2^{s.ocean}$ trends are parallel to or shallower than atmospheric trends over these long timescales. Cooling is found for most time series ending after 2002 in NP-SPSS, indicating that temperature and chemistry components are acting in opposition, with decreasing temperature trends being balanced by an increase in pCO_2-nonT. Warming trends occur for almost all time series in NP-STSS (Figure 5b), which reduces the pCO_2-nonT trend and thus suggests a reduced capacity for the update of carbon from the atmosphere. Trends with a start year of 1998 illustrate decreasing pCO_2-T trends due to the strong 1997–1998 El Niño event.

[35] For 1981–2010, both the North and South Pacific subtropical permanently stratified biome (NP-STPS and SP-STPS) $pCO_2^{s.ocean}$ trends are parallel to pCO_2^{atm} trends (Figures 5c, 5f, and 4b). Long-term $pCO_2^{s.ocean}$ trends are due primarily to changing chemistry (pCO_2-nonT) in both biomes. For timescales of 15 years or less in the NP-STPS and SP-STPS, $pCO_2^{s.ocean}$ trends transition from steeper to parallel to shallower as the start year moves into the mid-1990s to late 1990s. Warming in NP-STPS contributes to steeper trends between the early 1990s to early 2000s. In SP-STPS, cooling trends on timescales less than 15 years contribute to some shallower trends.

[36] Due to intense upwelling, the tropical Pacific is a source of CO_2 to the atmosphere [*Feely et al*., 2006; *Takahashi et al*., 2009]. Analysis of trends in the equatorial Pacific Ocean was done with a 6 month shift (i.e., trends calculated from July to June rather than from January to December) in order to better capture ENSO influences. Additionally, for the western equatorial region (PEQ-W), January and February 1989 were excluded, consistent with previous studies, due to anomalous cold upwelling where these observations were collected [*Takahashi et al*., 2003; *Feely et al*., 2006].

[37] In the eastern half of the Pacific equatorial biome (PEQ-E), $pCO_2^{s.ocean}$ trends are parallel to pCO_2^{atm} trends on the long term, indicating that this region is a long-term steady source of CO_2 to the atmosphere (Figures 4c and 5d). The same is true for shorter timescales; however, the influence of ENSO [*McKinley et al*., 2004; *Feely et al*., 2006] is discernible as time series shorten. Steeper pCO_2^{atm} trends and cooling pCO_2-T signals for time series with a start year of 1997/1998 are consistent with a recovery from this strong El Niño. In the western half (split at 160°W) of the Pacific equatorial biome (PEQ-W), parallel pCO_2^{atm} trends are found for all time series longer than 25 years, which suggests a steady carbon source (Figure 5e). In contrast, trends covering timescales of 15 years or less reveal a transition in $pCO_2^{s.ocean}$ trends from steeper to shallower as start years move into the 1990s, consistent with ENSO influences. An increasing pCO_2-T trend over these short timescales, which diminishes as longer timescales are considered, may also be a contributing factor in this shift.

3.2. Atlantic Ocean

[38] For 1981–2010, trends in the North Atlantic Ocean ice (NA-ICE), subtropical seasonally stratified (NA-STSS), and subtropical permanently stratified (NA-STPS) biomes, $pCO_2^{s.ocean}$ trends parallel pCO_2^{atm} trends, while in the Atlantic equatorial (AEQ) biome, shallower $pCO_2^{s.ocean}$ trends are evident (Figures 4b and 6). Warming temperatures contribute significantly to trends in $pCO_2^{s.ocean}$ on this longest timescale in the subtropical and equatorial Atlantic.

[39] The Takahashi database extends only to 80°N and thus does not include the entire Arctic Ocean. Data coverage is sparse even in the covered region, leading to poor confirmation for the North Atlantic ICE biome and allowing for only limited interpretation. Nevertheless, the available data indicate parallel $pCO_2^{s.ocean}$ trends on timescales greater than 25 years (Figure 6a). Similar constraints exist for the North Atlantic subpolar seasonally stratified (NA-SPSS) biome (Figure 6b), with many trends longer than 20 years not confirming. For the confirmed time series exceeding 25 years, $pCO_2^{s.ocean}$ are steeper than pCO_2^{atm} trends in NA-SPSS, while warming is significant for a majority of trends from the mid-1980s to the 2000s.

[40] In the North Atlantic seasonally stratified biome (NA-STSS), $pCO_2^{s.ocean}$ trends are similar to those in NA-SPSS; however, they more clearly illustrate trends parallel to pCO_2^{atm} trends on timescales of 25+ years, while on shorter timescales, there is more variability (Figures 4 and 6c). Both warming and cooling trends in pCO_2-T are apparent on short timescales, while only warming exists for time series extending 20+ years.

[41] In the subtropical gyre of the North Atlantic (NA-STPS), $pCO_2^{s.ocean}$ trends are mostly parallel to pCO_2^{atm} trends, but there is also evidence of shallower trends, particularly for end years after 2007 (Figure 6d). On timescales of 25+ years, parallel trends remain dominant (Figure 4c), while warming is found for the large majority of timescales [*McKinley et al*., 2011]. This biome also presents an opportunity to make connections between a more familiar time series of monthly $pCO_2^{s.ocean}$ values (Figure 2a) and the grid format (Figures 5–7). In Figure 2a, positive and negative anomalies exist around the fit harmonic. Consider, for example, the positive anomalies in 1993; these are reflected in the grid (Figure 6d) by $pCO_2^{s.ocean}$ trends shallower than atmospheric trends for many time series with 1993 as the start year. Additionally, shallower trends for end years 2009 and 2010 reflect the negative $pCO_2^{s.ocean}$ anomalies that can be seen in Figure 2a during these years.

[42] In the equatorial Atlantic biome (AEQ), $pCO_2^{s.ocean}$ trends spanning 25+ years are equally split between shallower than and parallel to pCO_2^{atm} trends, with warming influencing most time series ending after 2005 (Figure 6e). For timescales of less than 25 years, $pCO_2^{s.ocean}$ trends also vary between parallel and shallower. In the South Atlantic (SA-STPS), very limited data lead to few confirmed trends. For timescales of 15 years or less, $pCO_2^{s.ocean}$ trends are parallel to and shallower than pCO_2^{atm} trends, with some warming (Figure 6f).

[43] Results from the non-ICE North Atlantic biomes (NA-SPSS, NA-STSS, and NA-STPS) are not strictly identical to those presented in *McKinley et al*. [2011] despite the similar database and analysis. These differences are due to an improved quality control, the use of a different SST climatology, and very slight changes to the biome boundaries due to this changed SST climatology (section 2.2). The actual values of $pCO_2^{s.ocean}$ trends do not differ substantially between the two studies, but in some cases the uncertainty is reduced by the additional quality control such that the designation with respect to steeper, parallel, or shallower is altered. Model confirmation can also be slightly changed because different numerical models are used.

3.3. Indian Ocean

[44] On the longest timescale, $pCO_2^{s.ocean}$ trends in the Indian Ocean subtropical permanently stratified biome (IND-STPS) are parallel to pCO_2^{atm} (Figures 4b and 7a). With end years of 2008 and prior, steeper trends dominate. Warming contributes to many trends ending in 2008 or later.

3.4. Southern Ocean

[45] In the Southern Ocean subtropical seasonally stratified (SO-STSS) biome, 29 and 30 year trends in $pCO_2^{s.ocean}$ are

parallel to pCO_2^{atm} trends and are driven by chemical changes. However, for 25–28 year lengths, results fluctuate across shallower, parallel, and steeper (Figure 7b). Further south, data are more limited in the Southern Ocean subpolar biome (SO-SPSS), resulting in few confirmed trends for time series of 25+ years (Figure 7c). For time series that do confirm, long-term $pCO_2^{s.ocean}$ trends are parallel to pCO_2^{atm} trends and cooling is found for early 1980s start years. Cooling is even more pronounced in the Southern Ocean ice biome (SO-ICE) where it influences most $pCO_2^{s.ocean}$ trends (Figure 7d). For the few 25+ year time series that do confirm in SO-ICE, shallower $pCO_2^{s.ocean}$ trends are found. On shorter timescales of 15 years or less, trends transition from steeper to parallel and to shallower than pCO_2^{atm} trends, and there is cooling throughout.

4. Discussion

4.1. Climate Indices

[46] Transient behaviors in atmospheric planetary-scale waves and in ocean circulation generate anomalies in climate on annual to multidecadal timescales over large geographical regions. These large-scale climate patterns, or climate modes, provide a partial conceptual framework in which observed changes in the physical environment can be interpreted. In Figure 8, trends for five major indices are presented: Pacific Decadal Oscillation (PDO), El Niño/Southern Oscillation (ENSO), Southern Annular Mode (SAM), North Atlantic Oscillation (NAO), and Atlantic Multidecadal Variation (AMV). These are calculated with a fit of a linear trend to the normalized time series [*Lovenduski et al*., 2007]. It is striking that long-term (25+ years) trends in both ENSO and SAM are statistically indistinguishable from zero, while trends in PDO and NAO are weakly negative. Only the AMV illustrates strong long-term trends, consistent with its multidecadal nature [*Ting et al*., 2009].

4.2. Pacific Ocean

[47] In the North Pacific, the PDO is a dominant mode of climate variability [*Mantua et al*., 1997]. *McKinley et al*. [2006] showed with multiple numerical models that the PDO is positively correlated with increased CO_2 uptake and is the dominant mode of modeled variability in CO_2 uptake, explaining 10–38% of model variance for 15–60°N. The PDO shifted from positive in the 1980s and 1990s to negative in the 2000s (Figure 8a). In NP-SPSS, cooling is consistent with the disappearance of the negative PDO trend in the mid-2000s as a negative trend in PDO should be associated with positive SST anomalies. Utilizing much the same data as in this study, *Takahashi et al*. [2006] found large declines in $pCO_2^{s.ocean}$, as well as significant cooling, between the 1970s and 1980s in the central Bering Sea, a region included in NP-SPSS. Other $10° \times 10°$ regions analyzed by *Takahashi et al*. [2006] within this biome have $pCO_2^{s.ocean}$ trends parallel to pCO_2^{atm} trends and variable temperature trends. Our finding of cooling and shallow $pCO_2^{s.ocean}$ trends may be due to this same enhanced mixing and productivity in the Bering Sea.

[48] In NP-STSS, $pCO_2^{s.ocean}$ trends are generally parallel to pCO_2^{atm} trends, with the exception of mostly shallower trends for end years between 2007 and 2009. Warming is found throughout this biome, consistent with a shift toward a lower PDO index in the 2000s. This biome sits within a primary center of SST change for the PDO [*Mantua et al*., 1997], where a high (low) PDO index is associated with cold (warm) SST. *McKinley et al*. [2006] showed that in numerical models, the impact of the PDO on $pCO_2^{s.ocean}$ in this region depends primarily on the balance between SST change (negatively correlated with PDO) and dissolved inorganic carbon (DIC) change (positively correlated with PDO). Thus, the trend to lower $pCO_2^{s.ocean}$ in 2007–2009, along with a resumption of the negative PDO trend (Figure 8a), suggests that the impact of reduced DIC concentration is driving the pCO_2 response. Both biological drawdown and advection contribute to the removal of carbon from the surface waters, while wintertime vertical convergence is a contributing physical factor to the seasonal increase of winter $pCO_2^{s.ocean}$ in this region [*Ayers and Lozier*, 2012]. Warming may act to enhance stratification, damp vertical circulation, and thus reduce the mixing of high-DIC waters from below.

[49] In NP-STPS, trends vary considerably across timescales. Warming influences some time series, particularly from the 1990s to early 2000s, but there is no tendency toward a greater influence of warming as in the North Atlantic STPS [*McKinley et al*., 2011]. Trends for 1981–2004 are parallel to pCO_2^{atm}, consistent with *Takahashi et al*. [2006]. Shallower $pCO_2^{s.ocean}$ trends for end years 2005–2008 may be connected to this period having a lull in the PDO trend; a negative PDO trend is associated with a basin-wide positive tendency in $pCO_2^{s.ocean}$ [*McKinley et al*., 2006].

[50] Trends in $pCO_2^{s.ocean}$ calculated from TCO_2, SST, ALK, and SSS, collected at station ALOHA as part of the Hawaii Ocean Time series (HOT) program (Figure 9a), agree to a large degree with NP-STPS results. *Dore et al*. [2003] reported a decreasing carbon sink for measurements at station ALOHA for a 13 year timescale (1989–2001) with temperature playing an insignificant role in the trend, consistent with our results for the entire NP-STPS biome (Figure 5c). Further work by *Dore et al*. [2009] reports a transition to steady carbon uptake at station ALOHA when data are extended to 2007. This shift from shallower to parallel trends generally agrees with our findings for the NP-STPS (Figure 5c). Though results are not exactly the same between HOT and NP-STPS, this comparison suggests that HOT is reasonably representative of the North Pacific subtropical gyre with respect to $pCO_2^{s.ocean}$ variability.

[51] In the east equatorial Pacific (Figure 5d), trends in $pCO_2^{s.ocean}$ are steeper than pCO_2^{atm} and there is cooling for start years including 1997 due to recovery from the very strong 1997–1998 El Niño (Figure 8b) that caused low $pCO_2^{s.ocean}$ and warm surface temperatures [*Feely et al*., 2006]. Some cooling is also found for the early 1990s to the late 2000s, consistent with the analysis of satellite data that indicates a large-scale shift of the mean state of the equatorial Pacific toward cooler in the east and warmer in the west during the 2000s [*McPhaden et al*., 2011]. Otherwise, $pCO_2^{s.ocean}$ trends are largely parallel to pCO_2^{atm} trends as time series lengthen, which is consistent with trends in ENSO fading away on timescales longer than 20 years (Figure 8b).

[52] In the west Pacific equatorial biome (Figure 5e), $pCO_2^{s.ocean}$ trends are shallower than pCO_2^{atm} trends for start years 1995–1996 and 1998–1999 through 2010–2011, due to these short time series being influenced by high-pCO_2

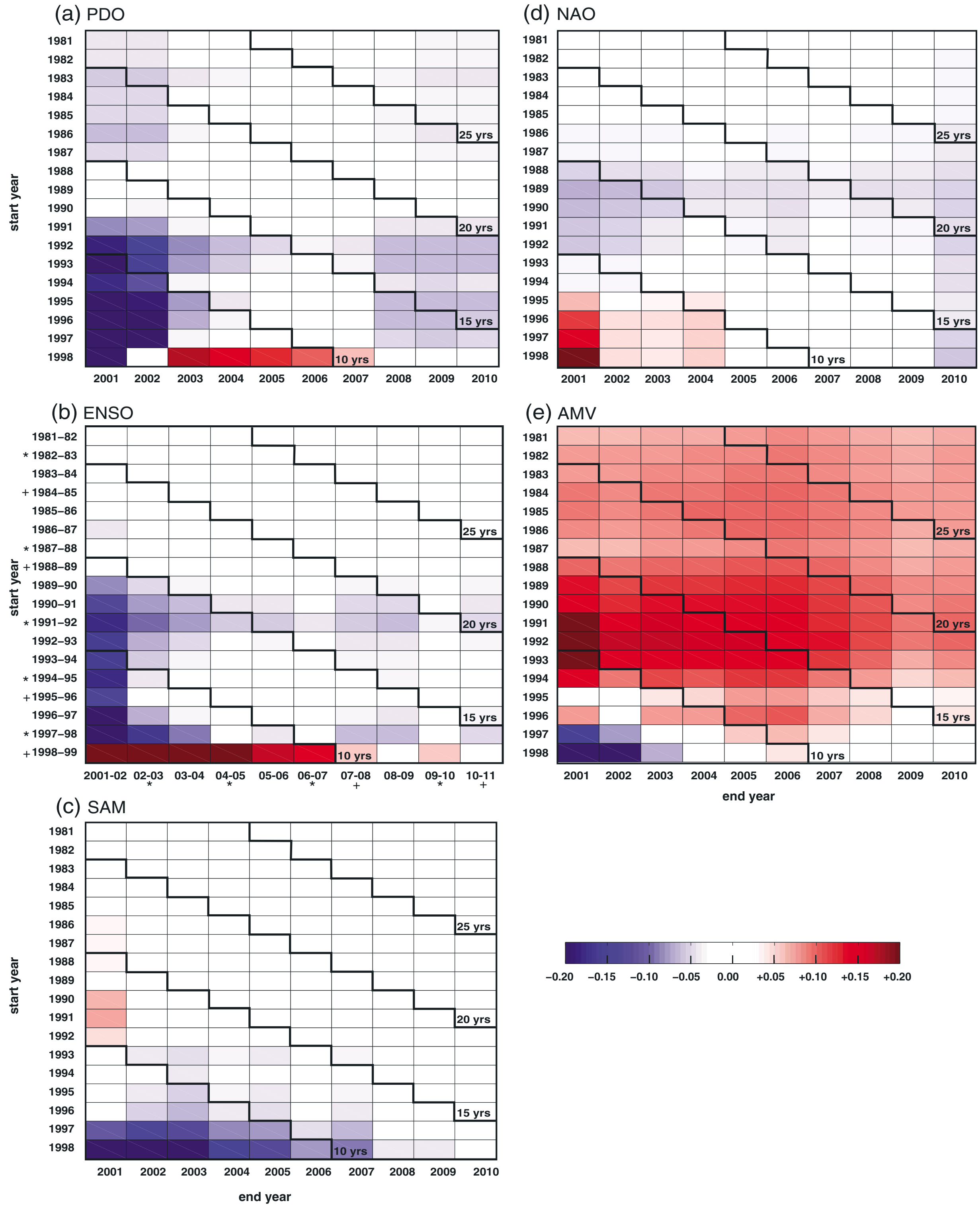

Figure 8. Linear trends in normalized climatic indices, with variable years: (a) Pacific Decadal Oscillation (PDO), (b) El Niño/Southern Oscillation (ENSO), (c) Southern Annular Mode (SAM), (d) North Atlantic Oscillation (NAO), and (e) Atlantic Multidecadal Variation (AMV). Dark blue for trends less than zero; red for larger than zero given 1σ uncertainties which range from 0.025 to 0.05.

La Niña conditions in the start years (Figure 8b). For the end years of 2001–2002, $pCO_2^{s.ocean}$ trends are steeper than pCO_2^{atm} because of the extended 1998–2001 La Niña toward the end of these time series. There is a dominance of warming trends, consistent with findings of *McPhaden et al.* [2011], though some cooling is also found for time series starting in the mid-1980s. As time series lengthen, trends are largely parallel to atmospheric trends.

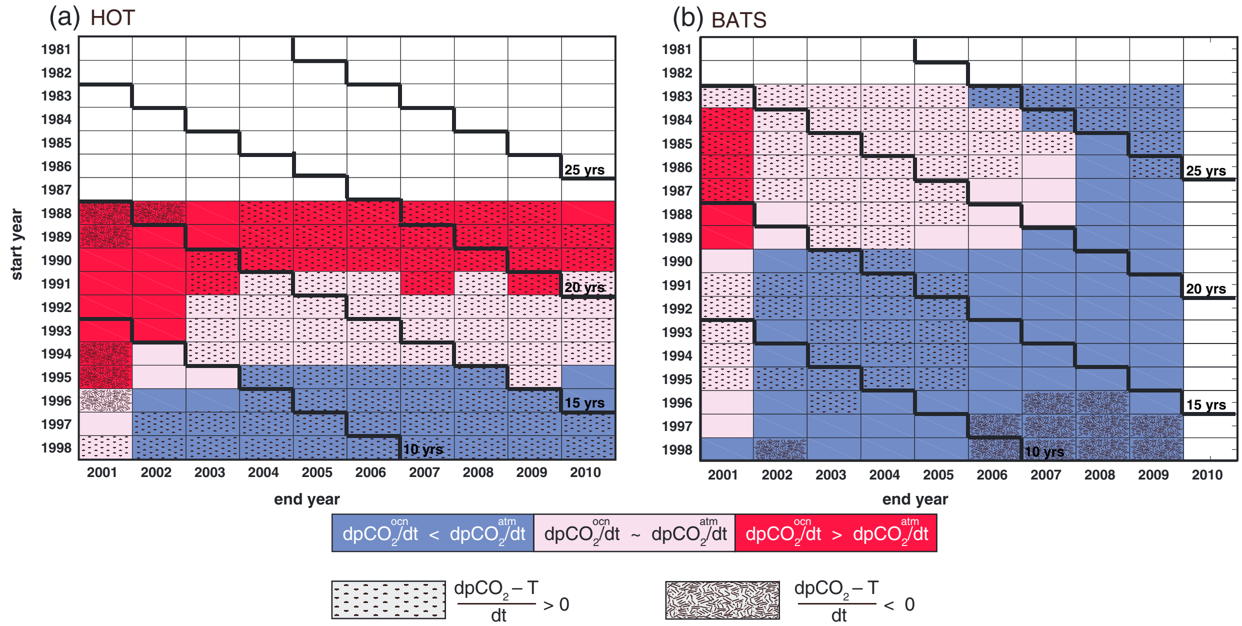

Figure 9. Trend in $p\mathrm{CO}_2^{\mathrm{s.ocean}}$ versus $p\mathrm{CO}_2^{\mathrm{atm}}$ trend, with variable start and end years for (a) Hawaii Ocean Time series (HOT) in the subtropical Pacific and (b) Bermuda Atlantic Time series Study (BATS) in the subtropical Atlantic. Colors and stippling as in Figure 4. White indicates data not available.

[53] In the South Pacific STPS biome, $p\mathrm{CO}_2^{\mathrm{s.ocean}}$ trends are shallower than $p\mathrm{CO}_2^{\mathrm{atm}}$ trends on timescales longer than 25 years. Previous studies using observations in the western half of the biome concur with shallower $p\mathrm{CO}_2^{\mathrm{s.ocean}}$ trends [*Inoue and Ishii*, 2005; *Le Quéré et al.*, 2009]. Temperature trends in this region remain indistinguishable from zero on long timescales; however, cooling trends have been significant for shorter time series ending in the early 2000s to mid-2000s, possibly due to PDO and ENSO effects (Figures 8a and 8b).

4.3. Atlantic Ocean

[54] The lack of data in the North Atlantic ice biome (NA-ICE) leads to many time series that do not confirm with the model-based test. This is a complex, rapidly changing region, and thus, trends are difficult to discern [*Schuster et al.*, 2012]. Confirmed trends for 1981–2010 do show $p\mathrm{CO}_2^{\mathrm{s.ocean}}$ trends parallel to $p\mathrm{CO}_2^{\mathrm{atm}}$ trends (Figures 6a and 4b), which is consistent with a previous analysis of much of the same data [*Le Quéré et al.*, 2009]. Trends on shorter timescales are quite sensitive to the start/end year pair, which suggests significant variability. With the exception of trends starting in 1995–1996, no significant influence of warming is found; on the contrary, we see signals of significant cooling between the 1980s and the early 2000s to mid-2000s. Ongoing projects such as CARINA [*Olsen et al.*, 2009] will increase data density and improve trend confidence in future studies.

[55] Trend confirmation is also an issue in the North Atlantic subpolar biome (NA-SPSS) where over 50% of trends longer than 25 years do not confirm. For confirmed trends of 25+ years (up to an end year of 2007), we find $p\mathrm{CO}_2^{\mathrm{s.ocean}}$ trends steeper than $p\mathrm{CO}_2^{\mathrm{atm}}$. Results for the early 1980s through the early 2000s are consistent with a previous study that found steeper $p\mathrm{CO}_2^{\mathrm{s.ocean}}$ trends for 1982–1998 in this region [*Lefèvre et al.*, 2004]. Additionally, for the mid-1990s to the 2000s, $p\mathrm{CO}_2^{\mathrm{s.ocean}}$ trends are steeper than $p\mathrm{CO}_2^{\mathrm{atm}}$, consistent with the results of *Corbière et al.* [2007] in the SURATLANT region between Iceland and Newfoundland for 1993–2003 and of *Metzl et al.* [2010] when extending to 2007. For trends starting in the 1990s and ending in 2008–2010, we find shallower $p\mathrm{CO}_2^{\mathrm{s.ocean}}$ trends, which contrasts with *Metzl et al.* [2010] who found acceleration in the growth rate of wintertime $p\mathrm{CO}_2^{\mathrm{s.ocean}}$ in the late 2000s in the SURATLANT region. This wintertime acceleration may not have been a biome-wide phenomenon and/or not acted across the full annual cycle.

[56] Changes in the subpolar circulation and convective mixing in response to climatic variability have been identified in previous modeling studies for the period 1992–2006 [*Ullman et al.*, 2009], and connections to NAO variability have been made within the time frame of 1979–2004 [*Thomas et al.*, 2008]. Between the mid-1990s and mid-2000s, the NAO transitioned from a strong positive to a neutral or slightly negative phase and, at the same time, the longer-term AMV transitioned from a negative to a positive phase (Figures 8d and 8e) [*Ting et al.*, 2009; *Hurrell and Deser*, 2010; *Häkkinen et al.*, 2011]. However, for longer timescales, NAO trends fade away while AMV trends continue to be strong. The warming trend over most time series in NA-SPSS has previously been attributed to a combined effect of this AMV trend and an anthropogenic warming [*Ting et al.*, 2009; *Löptien and Eden*, 2010].

[57] In the North Atlantic subtropical seasonally stratified biome (NA-STSS), the trend pattern is similar to that in the NA-SPSS, which suggests that interannual to multidecadal variability in both biomes is linked to changes in circulation and horizontal advection in response to climatic variability [*Thomas et al.*, 2008; *Ullman et al.*, 2009]. Steeper than atmospheric $p\mathrm{CO}_2^{\mathrm{s.ocean}}$ trends in the late 1980s to the early 2000s to mid-2000s are consistent with the findings of *Schuster et al.* [2009] using a variety of data sets with variable lengths to construct estimates for 1990–2006 trends. In NA-STSS, warming and cooling both influence trends,

with cooling appearing for a few time series less than 15 years (Figure 6c). A clear tendency to a greater influence of warming for longer time series is not found.

[58] In the North Atlantic subtropical permanently stratified biome (NA-STPS), signals of decadal variability are less prevalent, such that $pCO_2^{s.ocean}$ trends are parallel to pCO_2^{atm} trends for most time series (Figure 6d). Exceptions are for trends ending after 2008, where shallower trends are predominantly found. *Schuster et al*. [2009] found a shallower than atmospheric trend in this region for 1990–2006. Together, these results suggest that 2006 may have been a time of transition toward shallower trends. For all time series longer than 20 years, both warming and chemistry drive $pCO_2^{s.ocean}$ trends [*Le Quéré et al*., 2010; *McKinley et al*., 2011].

[59] Biome-scale results do not preclude the existence of differing trends at smaller spatial scales, and we can directly address this comparison in NA-STPS using the Bermuda Atlantic Time series Study (BATS) data, which are not included in our biome analysis. Results from BATS for 1983–2009 do indicate some differences (Figures 6d and 9b), but the same overall conclusions are derived from BATS as for the whole NA-STPS for 1983–2009: shallower than atmospheric trends for time series ending in the late 2000s and a statistically significant influence of warming on many timescales. Similar to results for HOT and NP-STPS, this comparison with an independent data set also confirms previous modeling-based results [*McKinley et al*., 2004] that the BATS time series is reasonably representative of the subtropical gyre.

[60] Across timescales in both the NA-SPSS and NA-STPS biomes, warming is a contributing mechanism for $pCO_2^{s.ocean}$ trends, and this warming does not decay away at the longest time series (Figures 6b and 6d), suggesting a reduced capacity for carbon uptake due to warming [*Sarmiento and Le Quéré*, 1996; *Le Quéré et al*., 2010; *McKinley et al*., 2011]. As discussed for NA-SPSS, this warming has previously been shown to be due partially to anthropogenic forcing and partially to the AMV [*Ting et al*., 2009; *Löptien and Eden*, 2010]. In NA-STSS, there is spotty evidence of warming (Figure 6c), but since it does not become more prevalent for later end years, we conservatively interpret this as evidence of decadal variability as opposed to a clear signal of long-term warming.

[61] The equatorial region of the Atlantic Ocean (AEQ) displays $pCO_2^{s.ocean}$ trends that are parallel to or shallower than pCO_2^{atm} trends on nearly all timescales. Due to equatorial upwelling, this region outgases CO_2 to the atmosphere [*Schuster et al*., 2012]. Long-term shallower trends are consistent with a $pCO_2^{s.ocean}$ lag due to dilution with this low-anthropogenic CO_2 water. Warming is found in AEQ, especially when trends are calculated through end years in the mid-2000s to the late 2000s (Figure 6e), also consistent with the AMV trend (Figure 8e) [*Ting et al*., 2011]. In the SA-STPS biome, a lack of observations makes for poor model confirmation, but for the confirmed time series, patterns have some similarity to AEQ (Figure 6f).

4.4. Indian Ocean

[62] Trends in $pCO_2^{s.ocean}$ are steeper than pCO_2^{atm} trends for most time series in the Indian Ocean subtropical permanently stratified biome (IND-STPS). *Metzl* [2009] used some of the same observations for 1991–2007 in a region south of 20°S, from 30 to 90°E, to find summertime steeper trends and wintertime parallel trends, with the proposed mechanism being enhanced Southern Ocean upwelling of TCO_2 with the trend to positive SAM over this period. *Metzl* [2009] also found significant cooling, which we do not. The substantially different regions used are likely responsible for this difference. In our analysis for end years 2009 and 2010, there is a shift toward $pCO_2^{s.ocean}$ trends parallel to pCO_2^{atm} trends. This feature is largely independent of the start year (Figure 7a). Shallower trends for start years 1997–1998 may indicate a recovery from the 1997–1998 El Niño.

4.5. Southern Ocean

[63] The circulation and carbon cycle of the Southern Ocean has been shown to be affected by multiple climatic oscillations, particularly the Southern Annular Mode/Antarctic Oscillation (SAM/AAO) [*Thompson and Solomon*, 2002; *Le Quéré et al*., 2007; *Lovenduski et al*., 2007, 2008]. ENSO has also been shown to impact carbon cycling and biogeochemistry here [*McKinley et al*., 2004; *Lovenduski and Gruber*, 2005].

[64] *Lovenduski et al*. [2007] discussed Southern Ocean CO_2 fluxes in the context of four regions, and our biomes correspond to three of these. The Subantarctic Zone (SAZ), between the Subantarctic Front (SAF) and South Subtropical Front, corresponds to our SO-STSS biome. The Polar Frontal Zone, between the SAF and the Antarctic Polar Front (APF), corresponds to our SO-SPSS biome. The Antarctic Zone (AZ) south of the APF corresponds to our SO-ICE biome. *Lovenduski et al*. [2007, 2008] used an ocean biogeochemical model to study CO_2 flux variability, focusing on the period 1979–2004. They found a significant enhancement in the outgassing of natural CO_2 during positive anomalies in the SAM in all three zones; in the SO-ICE/AZ and SO-SPSS/APF, there is also an increase in the uptake of anthropogenic CO_2 that, to a small degree, offsets the enhanced outgassing. The net effect of a positive SAM tendency is less carbon taken up from the atmosphere. A positive SAM trend has been cited as the reason for decreasing Southern Ocean carbon uptake and driving an enhanced growth rate of atmospheric CO_2 through the mid-2000s [*Canadell et al*., 2007; *Le Quéré et al*., 2007]. In this analysis, a positive SAM trend appears only from the late 1980s and early 1990s to 2001. The positive SAM trend disappears after 2001 (Figure 8c), and short-term trends from the mid-1990s to the 2000s have actually been negative. For most time series longer than 18 years, the SAM trend has been statistically indistinguishable from zero (Figure 8c). These results are unchanged if an alternative SAM index is used (section 2.2). Next we will investigate the relationships to trends in $pCO_2^{s.ocean}$.

[65] In the SO-STSS/SAZ biome, ocean carbon trends vary across the available time series, such that long-term $pCO_2^{s.ocean}$ trends parallel to pCO_2^{atm} trends have not yet become predominant for timescales exceeding 25 years (Figures 4c and 7b). There is some warming specifically with end years 2007–2009, but it is not clearly increasing on long timescales. The elucidation of impacts from trends in the SAM index is difficult because there is generally insufficient pCO_2 data in the years when the SAM has significant trends. While we do find $pCO_2^{s.ocean}$ trends steeper than atmospheric trends for time series from the 1980s to the mid-2000s, consistent with the proposed mechanism of enhanced

upwelling of natural carbon, we do not find significant positive trends in the SAM over this period (Figure 8c) [*Le Quéré et al.*, 2007; *Lovenduski et al.*, 2007, 2008]. Shallower trends do appear between the 1990s through 2009–2010, which is consistent with a weak negative tendency in the SAM from l998 to 2009, as well as an observed slackening of surface winds in reanalyses over 40–60°S (T. Ito, personal communication, 2012). Overall, we find that trends in the SAM do not extend past the early 2000s and thus have not been a significant driver of SO-STSS $pCO_2^{s.ocean}$ trends on timescales longer than 15 years.

[66] In the SO-SPSS/APF biome, for time series with end years up to 2007, $pCO_2^{s.ocean}$ trends are largely parallel to trends in pCO_2^{atm}, and a cooling trend emerges for trends beginning in the early 1980s (Figure 7c). Though we do not find significant trends in the SAM over this period, if the cooling is being driven by enhanced upwelling [*Metzl*, 2009; *Ito et al.*, 2010], it appears that any additional carbon being supplied is being ventilated to the atmosphere under the influence of the region's high winds. On shorter timescales, there are some $pCO_2^{s.ocean}$ trends steeper than pCO_2^{atm} trends, as well as cooling, through time series ending in 2002. There are also warming and shallower $pCO_2^{s.ocean}$ trends for time series starting after 1993. Both of these signals are consistent with the positive SAM/enhanced upwelling (negative SAM/decreased upwelling) of natural carbon mechanism, but again we note that these only appear in time series of lengths shorter than 15 years.

[67] In SO-ICE/AZ, $pCO_2^{s.ocean}$ trends with end years of 2007 and later predominantly are shallower than trends in pCO_2^{atm} (Figure 7d) and are consistent with the 1986–2006 wintertime analysis by *Takahashi et al.* [2009] for waters with SST < 6.5°C. A shift to shallower trends after 2007 may have been driven by a decline in upwelling due to weakening Southern Ocean winds since a maximum in 1999 (T. Ito, personal communication, 2012). Cooling is a dominant signal across timescales in SO-ICE/AZ.

[68] Sparse data across the Southern Ocean make it difficult to clearly elucidate $pCO_2^{s.ocean}$ trends for many start/end year pairs and limit our ability to distinguish between impacts of decadal to multidecadal variability from long-term trends. Nevertheless, when we consider timescales longer than 25 years, we find evidence for $pCO_2^{s.ocean}$ trends steeper than pCO_2^{atm} trends only for some time series in SO-STSS/SAZ. Otherwise, this analysis indicates that the Southern Ocean surface carbon content is increasing at the same rate or more slowly than the atmosphere (Figure 4b). This, coupled with cooling in SO-ICE/AZ and SO-SPSS/APF, increasing CO_2 solubility, suggests that the CO_2 sink strengthened in the late 2000s, and a recovery from previously reported declines between the early 1980s and early 2000s [*Le Quéré et al.*, 2007; *Lovenduski et al.*, 2007, 2008].

5. Summary and Conclusions

[69] With 30 years of available data, we find that the $pCO_2^{s.ocean}$ across the globe is increasing at a rate consistent with, or slightly below, the atmospheric rate of increase. In the Northern Hemisphere, long-term trends in $pCO_2^{s.ocean}$ tend to be parallel to pCO_2^{atm} trends. Biomes in the Southern Hemisphere show a greater tendency to shallower $pCO_2^{s.ocean}$ trends, though sparse data are a concern (Figure 4b). On decadal timescales, signals of variability abound (Figures 4a and 5–7), and there are indications of influence from climatic oscillations such as PDO, ENSO, SAM, NAO, and AMV. However, these signals fade away as timescales lengthen, with the exception of PDO and AMV that continue to have influence on the longest timescales (Figures 4b and 8).

[70] In equatorial and subtropical latitudes, 5 of 11 biomes have a majority of time series longer than 25 years that are both confirmed and that offer a consistent picture of $pCO_2^{s.ocean}$ trends (Figure 4c). In the Pacific, both equatorial biomes (PEQ-E and PEQ-W) consistently indicate $pCO_2^{s.ocean}$ trends parallel to pCO_2^{atm} trends, while SP-STPS has shallower trends. In the Atlantic, both NA-STSS and NA-STPS $pCO_2^{s.ocean}$ tend to parallel pCO_2^{atm} trends. In tropical and subtropical biomes that do not have consistent trends for 25+ years, data sparsity is the dominant problem (PEQ-W, NP-STSS, NP-STPS, SA-STPS, and IND-STPS). The equatorial Atlantic and SO-STSS are the only subtropical regions that do mostly confirm, but do not offer a consistent pattern of $pCO_2^{s.ocean}$ trends, suggesting that long-term climate variability continues to influence time series beyond 25 years. However, we do not find evidence that changes in the SAM drive this variability in SO-STSS.

[71] For the higher latitudes, no biome has enough data to offer a clear picture of 25+ years trends in $pCO_2^{s.ocean}$. More data are needed across the global ocean, and the next release of SOCAT, updated through 2010 (expected in June 2013) (B. Pfeil et al., A uniform, quality controlled Surface Ocean CO_2 Atlas (SOCAT), submitted to *Earth System Science Data Discussions*, 2012), should have up to 50% more data globally and will certainly improve our understanding of these biome-scale trends. Sustained data collection into the future is critical for the continued monitoring of the ocean carbon sink.

[72] As made evident by this work, only in a few regions of the ocean are data sufficient to determine trends in surface ocean pCO_2 parallel to the atmosphere (Figure 4c). The clearer signals are of substantial interannual to multidecadal timescale variability (Figures 4a and 5–7). Whether the longest timescale trends are considered over only 1981–2010 (Figure 4b) or for all time series longer than 25 years (Figure 4c), we find only $pCO_2^{s.ocean}$ trends parallel to or shallower than pCO_2^{atm} trends and no steeper trends. Parallel trends are consistent with basic thermodynamics and a long-term approximately steady state ocean circulation and carbon cycle. Shallower trends tend to occur in regions where there is substantial connection of the surface to deep waters, largely through Southern Ocean or equatorial upwelling, which is consistent with an injection to the surface of deep waters containing little anthropogenic carbon and, through this, a dampening of the rate of increase in $pCO_2^{s.ocean}$.

[73] Previous studies [e.g., *Metzl et al.*, 2010; *Schuster et al.*, 2009; *Le Quéré et al.*, 2009] have interpreted $pCO_2^{s.ocean}$ trends steeper than pCO_2^{atm} trends as indicative of a reduction in the ocean carbon sink. However, this interpretation has not accounted for the fact that $pCO_2^{s.ocean}$ not only drives the CO_2 sink (via ΔpCO_2) but also responds to the air-sea CO_2 flux. The fact that there is a chemical tendency to equilibrium between the atmosphere and ocean means that, even in the presence of climate feedbacks damping ocean carbon uptake, $pCO_2^{s.ocean}$ trends should parallel pCO_2^{atm} trends on long timescales. Further, both warming and carbon

uptake can drive change in $pCO_2^{s.ocean}$. We propose that a positive pCO_2-T trend, statistically distinguishable from zero, is a useful indicator for a negative feedback on ocean carbon uptake via surface ocean warming. Additional tests are needed to capture changes in the ocean carbon sink due to changing ocean circulation, particularly the surface to deep ocean exchange that ultimately allows the ocean to be the long-term modulator of anthropogenic CO_2 emissions on decadal to millennial timescales.

[74] The increasing influence of warming on $pCO_2^{s.ocean}$ trends is most clear in the subtropical North Atlantic (NA-STPS; Figures 4b and 4c) and is due to a long-term trend in the AMV and anthropogenic climate warming [*Loptien and Eden*, 2010; *Ting et al*., 2009]. These influences are consistent with the model-based analysis of the response of the ocean carbon cycle to observed warming in recent decades [*Le Quéré et al*., 2010], earlier idealized predictions [*Sarmiento and Le Quéré*, 1996], and projections with coupled carbon-climate models [*Roy et al*., 2011]. Consistent with our earlier findings [*McKinley et al*., 2011], this is observational evidence of a negative feedback from anthropogenic climate change on the ocean carbon sink in which warming reduces the carbon sink by driving a portion of the $pCO_2^{s.ocean}$ increase without carbon accumulation from the atmosphere.

[75] **Acknowledgments.** This work was supported by NASA grants (contracts 07-NIP07-0036, NNX/11AF53G, and NNX/13AC53G) and UW-Madison's SSEC. We thank T. Takahashi for his foresight and dedication, without which the $pCO_2^{s.ocean}$ database would not exist. We are grateful to C. Sabine and R. Feely (NOAA PMEL), P. Guttorp (U. Washington), and D. Polzin (UW-Madison) for the discussion and assistance. We thank A. Jacobson and K. Steinkamp for the comments and E. Sundquist and an Associate Editor for their editorial efforts.

References

Antonov, J. I., R. A. Locarnini, T. P. Boyer, A. V. Mishonov, and H. E. Garcia (2006), World Ocean Atlas 2005, vol. 2, Salinity, in *NOAA Atlas NESDIS 62*, edited by S. Levitus, 182 pp., U.S. Gov. Print. Off., Washington, D. C.

Assmann, K. M., M. Bentsen, J. Segschneider, and C. Heinze (2010), An isopycnic ocean carbon cycle model, *Geosci. Model Dev.*, *3*, 143–167.

Ayers, J. M., and M. S. Lozier (2012), Unraveling dynamical controls on the North Pacific carbon sink, *J. Geophys. Res.*, *117*, C01017, doi:10.1029/2011JC007368.

Bates, N. R. (2007), Interannual variability of the oceanic CO2 sink on the subtropical gyre of the North Atlantic Ocean over the last 2 decades, *J. Geophys. Res.*, *112*, C09013, doi:10.1029/2006JC003759.

Bennington, V., G. A. McKinley, S. Dutkiewicz, and D. Ullman (2009), What does chlorophyll variability tell us about export and CO2 flux variability in the North Atlantic?, *Global Biogeochem. Cycles*, *23*, GB3002, doi:10.1029/2008GB003241.

Böning, K., et al. (2008), The response of the Antarctic Circumpolar Current to recent climate change, *Nat. Geosci.*, *1*, 864–869, doi:10.1038/ngeo362.

Buitenhuis, E., R. Rivkin, S. Sailley, and C. Le Quéré (2010), Global biogeochemical fluxes through microzooplankton, *Global Biogeochem. Cycles*, doi:10.1029/2009GB003601.

Canadell, J. G., et al. (2007), Contributions to accelerating atmospheric CO2 growth from economic activity, carbon intensity, and efficiency of natural sinks, *Proc. Natl. Acad. Sci. USA*, *104*, 18, 866–18, 870, doi:10.1073pnas.0702737104.

Canadell, J. G., et al. (2011), An international effort to quantify regional carbon fluxes, *Eos. Trans. AGU*, *92*(10), 81–82, doi:10.1029/2011EO100001.

Corbière, A., N. Metzl, G. Reverdin, C. Brunet, and T. Takahashi (2007), Interannual and decadal variability of the oceanic carbon sink in the North Atlantic subpolar gyre, *Tellus, Ser. B*, *59*(2), 168–178, doi:10.1111/j.1600-0889.2006.00232.

Doney, S. C., V. J. Fabry, R. A. Feely, and J. A. Kleypas (2009), Ocean acidification: The other CO_2 problem. *Annu. Rev. Mar. Sci.*, *1*, 169–192.

Dore, J. E., R. Lukas, D. W. Sadler, and D. M. Karl (2003), Climate-driven changes to the atmospheric CO2 sink in the subtropical North Pacific Ocean, *Nature*, *424*, 754–757, doi:10.1038/nature01885.

Dore, J. E., R. Lukas, D. W. Sadler, M. J. Church, and D. M. Karl (2009), Physical and biogeochemical modulation of ocean acidification in the central North Pacific, *Proc. Natl. Acad. Sci. USA*, *106*, 12235–12240.

Feely, R., and C. Sabine (2007), Sea surface and atmospheric fCO_2 data in the Pacific Ocean during VOS project line onboard the R/V Ka'imimoana Cruises (2007). http://cdiac.ornl.gov/ftp/oceans/VOS_Kaimimoana/2007_data/. Carbon Dioxide Information Analysis Center, Oak Ridge National Laboratory, US Department of Energy, Oak Ridge, Tennessee. doi:10.3334/CDIAC/otg.VOS_Kaimimoana_2007.

Feely, R., and C. Sabine (2008), Sea surface and atmospheric fCO_2 data in the Pacific Ocean during VOS project line onboard the R/V Ka'imimoana Cruises (2008). http://cdiac.ornl.gov/ftp/oceans/VOS_Kaimimoana/2008_data/. Carbon Dioxide Information Analysis Center, Oak Ridge National Laboratory, US Department of Energy, Oak Ridge, Tennessee. doi:10.3334/CDIAC/otg.VOS_Kaimimoana_2008.

Feely, R. A., et al. (2006), Decadal variability of the air-sea CO_2 fluxes in the equatorial Pacific Ocean, *J. Geophys. Res.*, *111*, C08S90, doi:10.1029/2005JC003129.

GLOBALVIEW-CO2 (2010), Cooperative Atmospheric Data Integration Project—Carbon Dioxide, Reference Matrix. Earth Systems Research Lab, NOAA, Boulder, CO (ftp.cmdl.noaa.gov, Path: ccg/co2/GLOBALVIEW, NOAA ESRL, Boulder, CO).

Graven, H. D., T. P. Guilderson, and R. F. Keeling (2012), Observations of radiocarbon in CO2 at seven global sampling sites in the Scripps flask network: Analysis of spatial gradients and seasonal cycles, *J. Geophys. Res.*, *117*, D02303, doi:10.1029/2011JD016535.

Gruber, N., C. D. Keeling, and N. R. Bates (2002), Interannual variability in the North Atlantic Ocean carbon sink, *Science*, *298*, 2374–2378, doi:10.1126/science.1077077.

Gruber, N., et al. (2009), Oceanic sources, sinks, and transport of atmospheric CO2, *Global Biogeochem. Cycles*, *23*, GB1005, doi:10.1029/2008GB003349.

Häkkinen, S., P. Rhines, and D. Worthen (2011), Atmospheric blocking and Atlantic multidecadal ocean variability, *Science*, *334*, 655–659, doi:10.1126/science.1205683.

Hurrell, J. W., and C. Deser (2010), North Atlantic climate variability: The role of the North Atlantic Oscillation, *J. Mar. Syst.*, *78*. 28–41, doi:10.1016/j.jmarsys.2009.11.002.

Inoue, H. Y., and M. Ishii (2005), Variations and trends of CO_2 in the surface seawater in the Southern Ocean south of Australia between 1969 and 2002, *Tellus B*, *57* (1), 58–6, doi:10.1111/j.1600-0889.2005.00130.

Ito, T., M. Woloszyn, and M. Mazloff (2010), Anthropogenic carbon dioxide transport in the Southern Ocean driven by Ekman flow, *Nature*, *463*, 80–83.

Jones, S. D., C. Le Quéré, and C. Rödenbeck (2012), Autocorrelation characteristics of surface ocean pCO_2 and air-sea CO2 fluxes, *Global Biogeochem. Cycles*, *26*, GB2042, doi:10.1029/2010GB004017.

Keeling, C. D., and T. P. Whorf (2005), Trends: A Compendium of Data on Global Change, Carbon Dioxide Inf. Anal. Cent., Oak Ridge Natl. Lab., U.S. Dept. of Energy, Oak Ridge, Tenn.

Khatiwala, S., F. Primeau, and T. Hall (2009), Reconstruction of the history of anthropogenic CO_2 concentrations in the ocean, *Nature*, *462* (7271), 346–349, doi:10.1038/nature08526.

Khatiwala, S., et al. (2012), Global ocean storage of anthropogenic carbon, *Biogeosciences Disscuss*, *9*, 8931–8988, doi:10.5194/bgd-9-8931-2012.

Le Quéré, C., et al. (2007), Saturation of the Southern Ocean CO2 sink due to recent climate change, *Science*, *316*, 1735–1738, doi:10.1126/science.1136188.

Le Quéré, C., et al. (2009), Trends in the sources and sinks of carbon dioxide, *Nat. Geosci.*, *2*, 831–836, doi:10.1038/ngeo689.

Le Quéré, C., et al. (2010), Impact of climate change and variability on the global oceanic sink of CO2, *Global Biogeochem. Cycles*, *24*, GB4007, doi:10.1029/2009GB003599.

Lefèvre, N., et al. (2004), A decrease in the sink for atmospheric CO2 in the North Atlantic, *Geophys. Res. Lett.*, *31*, L07306, doi:10.1029/2003GL018957.

Lenton, A., et al. (2012), The observed evolution of oceanic pCO2 and its drivers over the last two decades, *Global Biogeochem. Cycles*, *26*, GB2021, doi:10.1029/2011GB004095.

Löptien, U., and C. Eden (2010), Multidecadal CO2 uptake variability of the North Atlantic. *J. Geophys. Res. 115*, D12113, doi:10.1029/2009JD012431.

Lovenduski, N. S., and N. Gruber (2005), Impact of the Southern Annular Mode on Southern Ocean circulation and biology, *Geophys. Res. Lett.*, *32*, L11603, doi:10.1029/2005GL022727.

Lovenduski, N., et al. (2007), Enhanced CO2 outgassing in the Southern Ocean from a positive phase of the Southern Annular Mode, *Global Biogeochem. Cycles*, *21*, GB2026, doi:10.1029/2006GB002900.

Lovenduski, N., N. Gruber, and S. C. Doney (2008), Towards a mechanistic understanding of the decadal trends in the Southern Ocean carbon sink, *Global Biogeochem. Cycles*, *22*, GB3016, doi:10.1029/2007GB003139.

Mantua, N. J., et al. (1997), A Pacific interdecadal climate oscillation with impacts on salmon production, *Bull. Am. Meteorol. Soc.*, *78*, 1069–1079.
Matear, R. J., and A. C. Hirst (2003), Long-term changes in dissolved oxygen concentrations in the oceans caused by protracted global warming, *Global Biogeochem. Cycles*, *17*(4), 1125, doi:10.1029/2002GB001997.
McKinley, G. A., M. J. Follows, and J. Marshall (2004), Mechanisms of air-sea CO2 flux variability in the equatorial Pacific and the North Atlantic, *Global Biogeochem. Cycles*, *18*, GB2011, doi:10.1029/2003GB002179.
McKinley, G. A., et al. (2006), North Pacific carbon cycle response to climate variability on seasonal to decadal timescales, *J. Geophys. Res.*, *111*, C07S06, doi:10.1029/2005JC003173.
McKinley, G. A., A. R. Fay, T. Takahashi, and N. Metzl (2011), Convergence of atmospheric and North Atlantic carbon trends on multidecadal timescales, *Nat. Geosci.*, doi:10.1038/ngeo119.
McPhaden, M. J., T. Lee, and D. McClurg (2011), El Niño and its relationship to changing background conditions in the tropical Pacific Ocean, *Geophys. Res. Lett.*, *38*, L15709, doi:10.1029/2011GL048275.
Metzl, N. (2009), Decadal increase of oceanic carbon dioxide in southern Indian surface ocean waters (1991–2007), *Deep Sea Res., Part II*, doi:10.1016/j.dsr2.2008.12.007.
Metzl, N., et al. (2010), Recent acceleration of the sea surface fCO_2 growth rate in the North Atlantic subpolar gyre (1993–2008) revealed by winter observations, *Global Biogeochem. Cycles 24*, GB4004, doi:10.1029/2009GB003658.
Olsen, A., et al. (2009), *Overview of the Nordic Seas CARINA data and salinity measurements Earth Syst. Sci. Data Discuss.*, *2*, 1–25.
Peters G. P., et al. (2011), Rapid growth in CO2 emissions after the 2008–2009 global financial crisis. *Nat. Clim. Change*, doi:10.1038/nclimate1332. Published online 4 December 2011.
Peylin, P., et al. (2005), Multiple constraints on regional CO2 flux variations over land and oceans, *Global Biogeochem. Cycles*, *19*, GB1011, doi:10.1029/2003GB002214.
Rayner, N. A., et al. (2003), Global analyses of sea surface temperature, sea ice, and night marine air temperature since the late nineteenth century, *J. Geophys. Res.*, *108*(D14), 4407, doi:10.1029/2002JD002670.
Roy, T., et al. (2011), Regional impacts of climate change and atmospheric CO2 on future ocean carbon uptake: A multimodel linear feedback analysis, *J. Climate*, *24*, 2300–2318, doi:10.1175/2010JCLI3787.1.
Sabine, C. L., et al. (2004), The oceanic sink for anthropogenic CO2, *Science*, *305*, 367–371, doi:10.1126/science.1097403.
Sarmiento, J. L., and C. Le Quéré (1996), Oceanic carbon dioxide uptake in a model of century-scale global warming, *Science*, *274*, 1346–1350, doi:10.1126/science.274.5291.
Sarmiento, J., et al. (2004), Response of ocean ecosystems to climate warming,*Global Biogeochem. Cycles*, *18*, GB3003, doi:10.1029/2003GB002134.
Schuster, U., and A. J. Watson (2007), A variable and decreasing sink for atmospheric CO2 in the North Atlantic, *J. Geophys. Res.*, *112*, C11006, doi:10.1029/2006JC003941.
Schuster, U., et al. (2009), Trends in North Atlantic sea surface fCO_2 from 1990 to 2006, *Deep Sea Res., Part II*, *56*:8–10, 620–629, doi:10.1016/j.dsr2.2008.12.011.
Schuster, U., et al. (2012), Atlantic and Arctic sea-air CO_2 Fluxes, 1990–2009, Biogeoscience Discussion, *9*, 10,669-10,724, doi:10.5194/bgd-9-10669-2012.
Smith, R. D., and P. R. Gent (2002), Reference manual for the Parallel Ocean Program (POP), ocean component of the Community Climate System Model (CCSM2.0 and 3.0), Tech. Rep. LA-UR-02-2484, Los Alamos National Laboratory. [Available online at http://www.ccsm.ucar.edu/models/ccsm3.0/pop].
Solomon, S. and Coauthors, Climate Change (2007), *The Physical Science Basis: Contribution of Working Group I to the Fourth Assessment Report of the Intergovernmental Panel on Climate Change*, Cambridge Univ. Press, Cambridge.
von Storch, H., and F. W. Zwiers (2002), *Statistical Analysis in Climate Research*, 484 pp., Cambridge Univ. Press, Cambridge, U. K.
Takahashi, T., et al. (2002), Global sea-air CO_2 flux based on climatological surface ocean pCO_2, and seasonal biological and temperature effects. *Deep-Sea Res*. *Ii 49*, 1601–1622.
Takahashi, T., S. C. Sutherland, R. A. Feely, and C. E. Cosca (2003), Decadal variation of the surface water pCO_2 in the western and central equatorial Pacific. *Science*, *302*, no. 5646, pp. 852-856, doi:10.1126/science.1088570.
Takahashi, T., S. C. Sutherland, R. A. Feely, and R. Wanninkhof (2006), Decadal change of the surface water pCO_2 in the North Pacific: A synthesis of 35 years of observations, *J. Geophys. Res.*, *111*, C07S05, doi:10.1029/2005JC003074.
Takahashi, T., and Coauthors (2009), Climatological mean and decadal changes in surface ocean pCO2, and net sea-air CO2 flux over the global oceans, *Deep Sea Res., Part II*, doi:10.1016/j.dsr2.2008.12.009.
Takahashi, T., S. C. Sutherland, and A. Kozyr (2011), ORNL/CDIAC-159, NDP-088. CDIAC, ORNL, U.S. DOE, Oak Ridge, TN, doi:10.3334/CDIAC/otg.ndp088(V2010).
Thomas, H., et al. (2008), Changes in the North Atlantic Oscillation influence CO2 uptake in the North Atlantic over the past two decades, *Global Biogeochem. Cycles*, *22*, GB4027, doi:10.1029/2007GB003167.
Thompson, D. W. J., and S. Solomon (2002), Interpretation of recent Southern Hemisphere climate change, *Science*, *296*, 895–899, doi:10.1126/science.1069270.
Ting, M., Y. Kushnir, R. Seager, and C. Li (2009), Forced and internal twentieth-century SST trends in the North Atlantic, *J. Clim. 22*, 1469–1481.
Ting, M., Y. Kushnir, R. Seager, and C. Li (2011), Robust features of Atlantic multi-decadal variability and its climate impacts, *Geophys. Res. Lett.*, *38*, L17705, doi:10.1029/2011GL048712.
Ullman, D. J., G. A. McKinley, V. Bennington, and S. Dutkiewicz (2009), Trends in the North Atlantic carbon sink: 1992–2006. *Global Biogeochem. Cycles 23*, GB4011, doi:10.1029/2008GB003383.
Watson, A. J., et al. (2009), Tracking the variable North Atlantic sink for atmospheric CO2, *Science*, *326*, 1391–1393, doi:10.1126/science.1177394.
Weiss, R. F., and B. A. Price (1980), Nitrous oxide solubility in water and seawater, *Mar. Chem.*, *8*, 347–359.
Wilks, D. S. (2006), *Statistical Methods in the Atmospheric Sciences*, 627 pp., Elsevier, Amsterdam.